Università degli Studi di Milano

PhD course in Biochemical Sciences, XXIX cycle

Department of Medical Biotechnology and Translational Medicine

SKELETAL MUSCLE AND CIRCULATING microRNAs IN MYOTONIC DYSTROPHY TYPE 1.

SDS: BIO/10

Alessandra Perfetti

ID: R10553

Supervisor: Prof. Luigi Anastasia

Coordinator: Prof. Sandro Sonnino

INDEX

VISUAL ABSTRACT

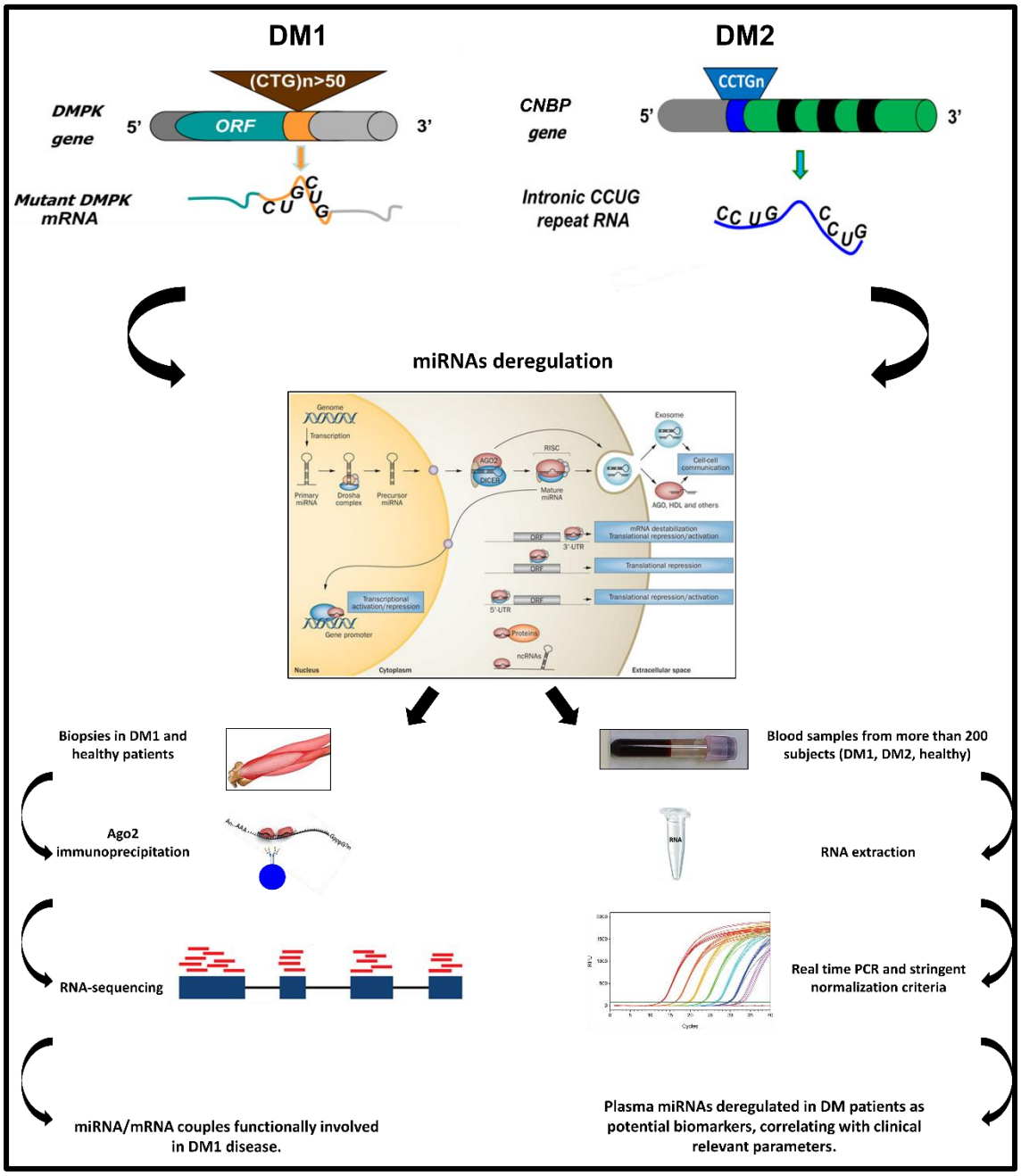

I. ABSTRACT

In Myotonic Dystrophy type 1 (DM1), the accumulation of transcripts containing CUG triplet expansions leads to the dysregulation of multiple cellular processes, including RNA splicing and microRNA (miRNAs) synthesis. This project aims to find functional miRNAs that are specifically deregulated in muscles of DM1 patients, and to identify circulating miRNAs in the plasma of DM1 patients that could be used as biomarkers of DM1 disease progression. Preliminary studies had previously identified a group of miRNAs that were deregulated in the plasma or serum of small groups of DM1 patients. In this work, very stringent selection and normalization criteria were adopted to validate or disprove these miRNAs in 103 DM1 patients and 111 matched controls. We found that 8 miRNAs out of 12 were significantly deregulated in DM1 patients and that the levels of these miRNAs discriminated DM1 from controls significantly. Next, we determined a "DM1-miRNAs score", calculated averaging the values of all 8 miRNAs, and a "miR-133a/b score" obtained averaging the levels of the two miR-133 members, both displaying a good ability to discriminate between DM1 and control subjects. Additionally, both scores correlated with muscle strength and Creatine Kinase levels. Moreover, 7 out of 8 miRNAs were found deregulated also in 30 patient affected by Myotonic Dystrophy type 2. The second aim of this work was the identification of miRNA/target mRNAs couples deregulated in skeletal muscles of DM1 patients. To this aim, the RNAs associated to RISC effector complex were analyzed from muscle biopsies of DM1 patients and healthy individuals and RNA-Sequencing was used to identify RISC-associated small RNAs (miRNAs) and long RNAs (mRNAs). A number of small and long RNAs differentially expressed in RISC complexes of DM1 vs healthy controls were identified, that showed statistically significant modulation. Next, using target prediction algorithms, miRNA-mRNA couples deregulated in DM1 were identified. RNA-sequencing data confirmed in independent qPCR assays, analyzing larger groups of DM1 patients and controls. Moreover, using myogenic cell models derived from dermal fibroblasts of DM1 patients and healthy individuals, a subset of these interactions was confirmed, validating this in vitro system for future functional studies.

In conclusion, this study identified relevant tissue miRNAs aberrantly expressed in DM1 and validated plasma miRNAs as potential DM1 biomarkers.

Abbreviations list.

DM = Myotonic dystrophy; CTR = control; CDM = congenital myotonic dystrophy; 3'UTR = 3' untranslated region; TP-PCR= triplet-repeat primed PCR; FISH = fluorescent in situ hybridization; IP= immunoprecipitations; RISC = RNA-induced silencing complex; MIRS= muscular impairment rating scale; MRC scale= medical research council scale; AUC = area under curve; CK= creatine kinase; ASO= antisense oligonucleotide; LNA= locked nucleic acid.

II. INTRODUCTION

II.I. MYOTONIC DYSTROPHIES

Myotonic dystrophies (DM) are autosomal dominant, multisystemic disorders sharing many clinical characteristics, including myotonia, progressive muscle weakness, heart conduction defects, posterior iridescent cataract and endocrine disorders [1,2]. To date, two different forms have been characterized: Myotonic Dystrophy type 1 (DM1, OMIM: 160900), also known as Steinert's disease, and Myotonic Dystrophy type 2 (DM2, OMIM: 602668), frequently indicated as Proximal Myotonic Myopathy (PROMM) or Proximal Myotonic Dystrophy (PDM).

Epidemiology of DM

DM1 prevalence estimates in Europe range from 1 in 8.300 to 1 in 10.700 [3], while studies performed on non-European populations indicate that DM1 is highly prevalent in certain founder populations like the one of Northeastern Quebec, where the frequency reaches 1 in 500 [4,5]. Prevalence of DM2 is thought to be underestimated, due to milder and ambiguous symptoms characterizing patients. Nevertheless, it is estimated to be similar to DM1 in European populations [6].

DM are repeated expansion diseases

DM1 is caused by $(CTG)_n$ expansions in the 3' untranslated region (UTR) of DMPK (*myotonic dystrophy protein kinase*) gene, which encodes for a myosin kinase ubiquitously expressed, but particularly relevant in skeletal muscle [2]. In the general population, CTG repeats range from 5 to 37 repeats, while DM1 patients present at least 50 and up to 4000 CTG repeats [7]. A mutation length of more than 2000 repeats causes the congenital form (CDM) [8], the most severe form of the disease, absent in DM2, with fetal onset and involvement of the central nervous system [9].

DM2 patients present $(CCTG)_n$ tetraplet repetitions in the first intron of the CNBP (*nucleic acid-binding protein)* gene [10]. The number of tetraplets is > 1000 in more than 90% of patients [5], while in healthy individuals the repeats are below 30 [11].

Both DM1 and DM2 mutations are characterized by high instability, leading to the so called "somatic mosaicism", due to the fact that certain tissues display a higher tendency to extend these tandem repeat sequences than others. As expected, the longest repeats are present in severely affected tissues: indeed, skeletal muscle cells possess considerably longer repeats than other cell types [1]. The genetic instability is also present in germline cells, which accumulate tandem repeats. Accordingly, DM is characterized by the genetic phenomenon of anticipation, so that symptoms begin at an earlier age in successive generations, especially in DM1 [12,13]. The congenital form of DM1 is almost always inherited by the mother [14]; however, anticipation may be also seen in patients with DM1 who inherited a smaller expanded CTG repeat from their father [15]. Finally, in DM2, there is the unusual tendency of repeats to be shorter in the offspring after both maternal and paternal transmission, with an increase in repeats size with age [16].

Clinical aspects

In DM1, distal skeletal muscles are generally more compromised, and the most severe type of DM1 is the CDM, which present a distinct clinical phenotype, in most cases even before birth. Respiratory failure is the main cause of post-natal death, but surviving babies present a gradual improvement in motor functions, and almost all CDM children are able to walk [2]. In the adult form of DM1, symptoms usually develop in the second, third or fourth decade [5] and distal muscle weakness, cataracts, myotonia, cardiac involvement and endocrine abnormalities are present in high percentage, with different grades [5,11]. Moreover, DM1 patients go through behavioral-personality changes (e.g., inactivity, apathic temperament and paranoid personality traits) and excessive daytime sleepiness [1].

Symptoms are generally milder in DM2 than in DM1, and usually begin in the second to sixth decade [16], selectively affecting the proximal muscles (limb girdle, neck flexor, and elbow extensor muscles) [5]. Myotonia is often less apparent in DM2 compared to DM1 [11], the cataracts have an appearance identical to that observed in DM1, and cardiac defects, like conduction abnormalities and arrhythmia, appear to be less severe and frequent in DM2 compared to DM1 [17].

DM patients seem to display higher risk of cancer, most frequently involving thyroid gland, ovary, colon, endometrium, brain, and eye (choriodal melanoma) [5,18,19], and very recently, it has been found that cancer risk seems to be sex-related, with a higher prevalence in DM1 females [20].

Furthermore, DM1 is frequently associated to metabolic dysfunctions, with insulin resistance, increased cholesterol and hypertriglyceridemia [21] and patients may also suffer of fertility dysfunction. Approximately two thirds of the affected males have reduced sperm quality as a result of testicular atrophy [22], while infertility in DM women is still debated [23], even if it was found that, especially in DM1, there is a reduced ovarian reserve, decreased embryo quality and lower live birth rates [24].

Mechanism of pathogenesis

For both DM1 and DM2, the expanded repetitions are present in non-coding sequences and both disorders result from toxicity of repetitive RNAs [25] with the mechanism of "toxic RNA gain-of-function" [26].

In DM1, the mutation is located near the site of polyadenylation but, even when the number of repeats is very high, it does not interfere with the processing of DMPK mRNA [5,26], which normally is spliced and polyadenylated. However, its nuclear sequestration in characteristic foci prevents translation.

A similar mechanism is involved in DM2 pathogenesis, where the transcribed but not translated CCUG in the first intron of the CNBP gene, leads to nuclear sequestration of the mRNA [27].

DMPK and CNBP mRNAs nuclear retention results in the sequestration of MBNL1 (*Muscleblind-1*) protein, which is one of the master regulators of the alternative splicing process [28], leading aberrant alternative splicing events of several transcripts [27]. Nuclear sequestration of mutated RNAs and their association to MBNL1 are easily detectable as foci [29] by fluorescent *in situ* hybridization (FISH) [30].

DMPK is a serine-threnonine kinase, whose role in skeletal muscle tissue is not yet well understood. It is associated to the nuclear envelope and its deficiency can cause nuclear envelope instability [31]. Harmon and colleagues also found that DMPK depletion reduces myogenin expression and prevents myotubes formation [32]; another study identified DMPK to be involved in the phosphorylation of the myosin-binding subunit of myosin phosphatase (MYPT1), which inhibits myosin phosphatase (PP1c) activity [1,33]. CNBP gene, on the other hand, is a nucleic acid binding protein which specifically binds to RNA and DNA, modulating the transcription of some genes involved in Wnt signaling [34], an important regulator of skeletal muscle development [35].

Despite the biological relevance of these genes, their haploinsufficency seems to be not the primary pathogenetic of DM. In fact, DMPK knockout mice do not reproduce the multisystemic phenotype

of DM1, and develop late-onset myopathy [36,37]. Regarding CNBP haploinsufficiency there are contrasting results: indeed, one study showed that CNBP +/- mice develop multisystemic features, like muscle wasting, cataracts and heart conduction defects [38]; however, another work showed that that CCTG expansion do not influence CNBP protein levels, dismissing decreased CNBP levels as pathogenetic mechanism [39].

MBNL1 is a part of a conserved protein family, composed by MBNL1, 2 and 3. All three members contain four CCCH zinc-finger protein domains, that are structured in pairs and function as RNA-binding domains [28]. MBNL proteins in normal cells act as alternative splicing regulators of several hundred transcripts [40] and they also have a role in regulating RNA transport and decay [41]. One of the MBNL1 characteristics is the high affinity with CUG repeats. This feature, in addition to mutated RNAs present in DM, leads to sequestration of MBNL1 into cell nuclei and to the misregulation of several splicing events [41]. In addition, the lack of MBNL1 bioavailability increases the activation of CUGBP1 (*CUG binding protein 1*), another splicing factor, which is more active in fetal life [26] (Figure1) These alterations lead to the maturation of fetal mRNA isoforms in DM adult tissues [42,43], potentially explaining many different symptoms present in DM. For example, the mis-splicing of ClC-1 (*Chloride channel 1*) correlates to reduced chloride conductance in skeletal muscle fibers, producing myotonia [44], while defects in the insulin receptor (IR) are associated to insulin resistance, frequently present in DM patients [45]. Several analyses of alternative splicing changes have been performed, also by our group [46–48], Indeed, the identification of aberrant splicing events not only can shed light on the disease mechanisms, but is also of potential prognostic use, since some events are present even before the appearance of symptoms [47].

Given the mounting evidence indicating splicing aberrations as a central disease mechanism, DM is often indicated as a "spliceopathy".

While aberrant alternative splicing is considered as the most plausible disease cause of DM, alternative mechanism have been proposed. Indeed, in 2010, Zu and colleagues discovered that in DM1, expansion mutations can drive the expression of proteins without an AUG initiation codon [49], and this novel type of translation was called *repeat associated non-ATG* (RAN) translation. Specifically, because DM1 mutation is bidirectionally [49], RAN translation of the DMPK antisense transcript gives rise to homopolymeric polyglutamine (poly$[Q]_n$) peptides in patients' cells, including skeletal muscle cells, and in mouse models of DM1[50].

Moreover, double-stranded $(CUG)_n$ hairpins are recognized by PKR (*dsRNA-activated protein kinase*) activating several cellular stress pathways, which finally lead to a global inhibition of

translation [51]. Accordingly, a significant reduction of protein synthesis has been reported both in DM1 and DM2 muscles, suggesting a functional link between reduced protein translation and muscle wasting [52,53]. Indeed, prolonged activation of PKR leads to stress in the endoplasmic reticulum, which could results in a block of translation initiation or apoptosis, both of which can lead to muscle wasting and weakness [50].

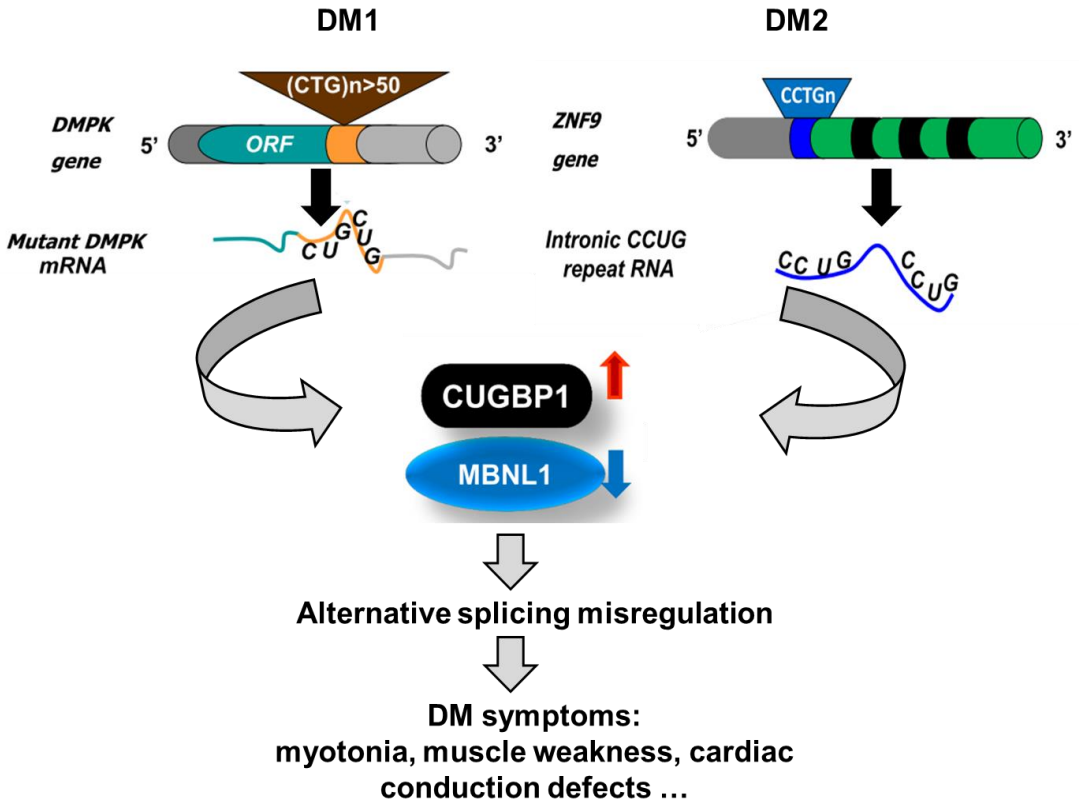

Figure 1. Pathogenetic mechanism in DM1 and DM2 Modified from[151]

Diagnosis and treatment

As for all genetic diseases with known mutations, also for DM1 and DM2 the typical diagnostic method is the genetic test. For DM1, PCR analysis is used to detect repeat lengths less than 100 and Southern blot analysis to detect larger expansions [2]. Triplet-repeat primed PCR (TP-PCR) [54] is also considered a routine diagnostic procedure, since it represents a robust and precise PCR method, but the association of two molecular methods such as Long-PCR and Southern transfer, together with TP-PCR [55,56], is strongly recommended to detect a wide range of mutations [2]. These analyses can be

performed using genomic DNA extracted from the peripheral blood, minimizing the invasiveness of the test.

For DM2, the presence of a wide variability in the clinical spectrum, makes the diagnosis more difficult. Furthermore, Southern blot and conventional PCR analysis are not suitable for a definitive genetic diagnosis, because of the extremely large size and somatic instability of the expansion mutation [10,57]. So, a more invasive, but conclusive method to obtain a DM2 diagnosis is represented by in situ hybridization (ISH), which is a method allowing the visualization of the mutant RNA in muscle tissues [58,59]. By using specific probes for CCUG expansions, it also permits a differential diagnosis between DM1 and DM2, [58,59]. Moreover, since MBNL1 is sequestered by mutant RNA foci, it is possible to visualize the nuclear accumulation of MBNL1 by FISH on muscle sections [2], even if it cannot distinguish between DM1 and DM2.

To date, no specific treatments are available for DM. Anti-myotonia therapy is helpful, and usually it consists in mexiletine or carbamazepine [2]; placement of a pacemaker or of a cardiac defibrillator can be lifesaving, especially in DM1 [5]. In general, the management of DM is based on preserving functions and independence, preventing cardiopulmonary complications and providing symptomatic treatments.

II.II. MicroRNAs IN TISSUES AND BODY FLUIDS

Biogenesis and function of microRNAs

MicroRNAs (miRNAs) are short (~23 nucleotides) non-coding RNAs, that play important gene regulatory roles in animals and plants by pairing to mRNA targets to lead their post-transcriptional repression. They are involved in virtually all biological process, including development, differentiation, stress response, apoptosis and proliferation [60].

The number of human miRNAs described to date has exceeded 2500, continuing to increase, and it is estimated that miRNAs regulate the expression of more 60% of protein-coding genes [61]. miRNA genes can be placed in independent transcription units or could be found in the introns of protein coding genes, and sometimes in exons of protein coding genes [62]. They are transcribed by RNA polymerase II, producing long capped and polyadenylated precursors called primary miRNAs (pri-miRNAs) [63,64]. The pri-miRNA contains a hairpin, of ∼70 nt (pre-miRNA), and the pre-miRNA, in turn, contains the sequence of the mature miRNA. Pre-miRNAs are processed by RNase III Drosha, in complex with the RNA-binding protein DGCR8 [65], and then exported by Exportin 5 to the cytoplasm [66], where it is further processed by RNase III Dicer in complex with the RNA-binding protein TRBP.

The resulting double stranded molecule of 22-23 nt associates to a protein of the Ago (*Argonaute*) family, which is the main component of the protein effector complex known as RISC (RNA-induced silencing complex). One of the strands of the duplex usually gets degraded, while the mature miRNA (guide strand) associates to the RISC complex, interacting with target mRNAs. The mechanism by which miRNA sequence complementarity drives the functional regulation of mRNA targets has been deeply investigated, finding that the miRNA 5′ region from nucleotide 2 to 8 (known as the 'seed' region) is of particular importance in targeting [67]. The seed region is the most evolutionarily conserved sequence of miRNAs [68] and its complementarity regions are more frequently found in the 3'UTR (3'-untranslated region) of the target mRNAs [69]. However, target sites in the 5'UTR (5'-untranslated region) or the coding region [70,71] are not uncommon.

In spite of intense research, the mechanisms through which miRNAs regulate gene expression remain unclear and have been subject of many controversies over the past few years. Indeed, evidence for both translational repression and mRNA destabilization has been shown [72]. First studies in animal cells pointed to regulation by miRNAs of mRNA translation. Translation in mammals requires many

factors allowing the recruitment of the ribosomal subunits to the mRNA initiation codon (initiation), the elongation of the nascent polypeptides (elongation) and the release of the mature protein (termination). Some of these factors recognize the 5' Cap or the 3' UTR of the mature mRNAs, allowing its efficient translation [73]. Many studies showed miRNAs ability to inhibit mRNA translation initiation [74,75]; however, elongation inhibition, premature termination of translation and co-translational protein degradation have been described as well [72,76–79]. While perfect pairing of a miRNA to its target, resulting in Ago2-dependent endonucleolitic cleavage, is seldom observed in animal cells, exonucleolitic degradation often occurs. miRNAs, promoting the recruitment of deadenylation factors to the target mRNA, stimulate the removal of mRNA poly-A tail, making it susceptible to exonucleolitic degradation. Indeed, binding of factors such as PAN2-PAN3 and CCR4-NOT [80], promotes deadenylation to repress translational initiation [81,82].

Many high throughput transcriptomic and proteomic studies all indicated that degradation of miRNA targets is a very common mechanism of miRNA action, providing a major contribution to target mRNA repression [60,72,83]. However, whether or not target degradation occurs as a consequence of an initial block in translation remains as an open issue.

There are also anecdotal reports of an activating role of the miRNAs: it has been described that they can cause an increase in mRNA translation (Vasudevan S., Tong Y. 2007). Moreover, epigenetically controlled transcriptional gene silencing has been identified as well [85].

Due to their short length and partial complementarity to mRNAs, each miRNA can regulates hundreds of targets [86]. On the other side, mRNAs usually have several binding sites for the same or different miRNAs, that provide a massive regulation of expression, which may be different in different cell types [87].

Indeed, each cell type has its specific miRNA expression profile, even if most miRNAs are expressed in several tissues, and only some of them have tissue-specific expression [88].

It is known that, for instance, miR-122 is typical of the liver [89], miR-126 is particularly enriched in the lung [90], miR-223 and miR-146a are more expressed in the spleen [90] and, finally, miR-1,-133a,-133b,-206, -208b, -486, -499 denote preferentially skeletal muscle and myocardial tissues, for this reason, they are indicated also as myomiRs [91,92]. These tissue specific miRNAs could play a role in key processes of development and function of individual tissues.

miRNAs in skeletal muscles

The potential of using miRNAs profiles for classification of skeletal muscle pathologies has been elegantly demonstrated by Kunkel's group, who identified distinct patterns of miRNAs in muscle biopsies derived from 10 major neuromuscular disorders [93]. We and others found that in DM1 muscles, miR-206, miR-1 and miR-335 are over-expressed, whereas miR-29b, miR-29c and miR-33 are down-regulated. However, independent studies have found either no changes in miR-1 levels or a reduction of this miRNA, due to defective maturation of the precursor [94–96]. In addition to miR-1, also miR-7 and miR-10 have been found downregulated in a DM1 Drosophila model as well as in DM1 patient-derived cells [94]. Importantly, we also found that miR-1, miR-133b and miR-206 myomiR intracellular distribution was severely altered [96].

Very recently, our group performed a study about skeletal myogenesis in mouse satellite cells, using *in silico* miRNA target prediction together with biochemical pull down techniques in order to obtain immunoprecipitates (IPs) of RISC complexes [97]. This approach, associated to RNA sequencing, have underlined the great importance of miR-222 in skeletal muscle differentiation; in particular, a new function of miRNA-222, leading to alteration of myogenesis at the level of the alternative splicing by Rbm24, was discovered [97]. Indeed, the RNA binding protein Rbm24 is a major regulator of muscle specific alternative splicing, and its down regulation by miRNA-222 resulted in defective exon inclusion, impairing the muscle-specific isoforms of Coro6 (*Coronin*), Fxr1(*FMR1 autosomal homolog 1*) and NACA (*nascent polypeptide-associated complex alpha subunit transcripts*) [97].

This study further underlines that, searching for "functional" miRNAs in muscle biopsies, i.e. of miRNA species actually associated to RISC complexes and engaged in mRNA targets downregulation, is of crucial importance to really understand the role of miRNAs in the pathogenetic process of skeletal muscle disorders.

Circulating miRNAs

miRNAs have been detected in most biological fluids, including plasma, serum, milk, tears, saliva, urine, amniotic, cerebrospinal and semen fluids [87]. These miRNAs are surprisingly very stable, showing distinct expression profiles among different fluids.

It is known that serum and other body fluids are rich in ribonucleases [98], but circulating miRNAs result to be very stable, because they are protected from degradation by the association with lipid

vescicles, with RNA-binding proteins [99], with high-density lipoproteins (HDL) or with Ago proteins [100,101] (Figure 2).

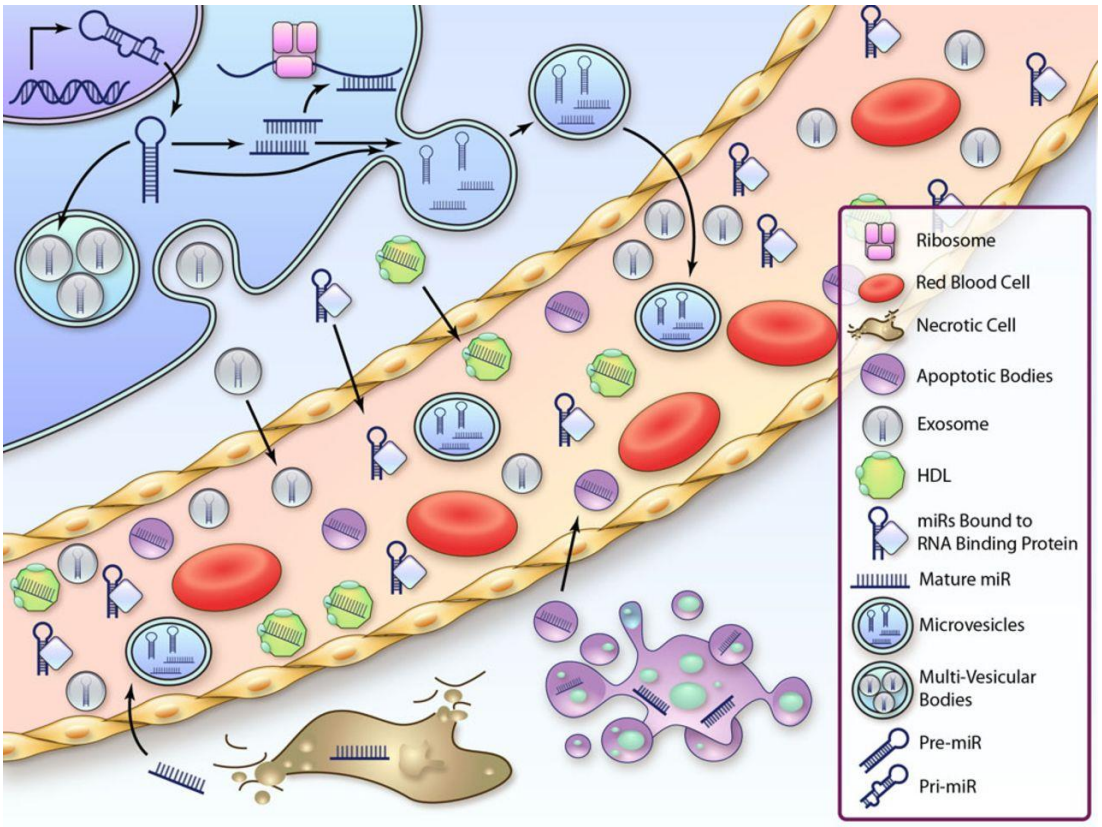

Figure 2. Circulating miRNAs [152]

Despite the growing number of evidence for the presence of miRNAs in body fluids, the origin and especially the function of these extracellular miRNAs are still poorly understood. Even if the presence of circulating miRNAs is probably a result of a combination between active and passive release by the cells, it is now clear that they have many characteristics to be good potential biomarkers. Moreover, given their specificity, another interesting possibility is to use circulating miRNA levels to monitor the physiopathological conditions of a specific organ [99].

The changes in circulating miRNA levels have been studied for several diseases, in different body fluids. For example, serum levels of miR-141 is able to discriminate between patients with advanced prostate cancer and healthy individuals [102], while miR-1, -133a/b, -208b and miR-499 are elevated in myocardial infarction and correlate with troponin plasma levels [103,104]. Moreover, circulating miRNAs were also found deregulated in muscular dystrophies: indeed, levels of muscle-specific miRNAs (myomiRs), like miR-1, -133a/b, -206 have been found altered in the blood of both mice and humans affected by Duchenne muscular dystrophy [105,106].

Very recently, two independent studies have identified plasma/serum circulating miRNA levels altered in small groups of DM1 patients [107,108]. In particular, the study of our group was conducted on plasma derived from 36 DM1 and 36 healthy subjects, finding 8 miRNAs (miR-133a, -193b, -191, -140-3p, -454, -574, -885-5p) increased and only 1 (miR-27b) decreased in DM1 [108]. Moreover, both miR-133a alone or the entire miRNA signature display an inverse correlation with muscle strength and show higher values present in more compromised patients [108]. In the study of Koutsoulidou et al., serum myomiRs (miR-1, -133a,-133b,-206) were found up-regulated in 23 DM1 and correlated to disease progression [107].

Biomarkers are critically important for disease diagnosis and monitoring. In particular, close monitoring of disease evolution is eminently required for the evaluation of therapeutic treatments. The ability to indicate the state of an organism, combined with high stability, make circulating miRNAs suitable markers allowing non-invasive and highly specificity diagnostics. This could help not only to save time and money, but also to be more accurate than using the existing markers [109].

Nevertheless, there are some issues which need to be resolved, in order to create standardized and reproducible procedures in the quantification of circulating miRNAs. One of the main problem is that, especially for rare diseases such as DM, most studies lack power because of small size of the patient groups analyzed. This limitation, associated to the great challenge in finding a robust normalization method, frequently lead to conflicting or not reproducible results.

Therapeutic modulation of miRNAs

Antisense Oligonucleotides (ASO) are the most used technology for inhibiting miRNAs. In particular, the use of Locked Nucleic Acid (LNA)-modified oligonucleotides is very frequent in *in vitro* and *in vivo* studies, given the high bio-stability, the low toxicity and good bio-distribution [110]. As previously mentioned, miR-122 is highly abundant in liver, and it has been demonstrated to be required for HCV (hepatitis C virus) replication [111], which is the major cause of hepatocellular carcinoma (HCC) in humans [111].

It has been found that, in chronically infected chimpanzee, the usage of LNA-anti-miR-122 reduced more than 300 fold the HCV levels in sera of animals treated with LNAs [112]. These results lead to consider miRNAs as efficient therapeutic targets also in humans, and a clinical trial on HCV infected patients with anti-miR-122 treatments (Miravirsen) successfully completed phase 2 [63]. These

results provide perspectives on the future of miRNA-based therapeutics for many other diseases, like cancer, cardiomyopathies and skeletal muscle dystrophies.

II.III. AIMS OF THE PROJECT

In the last decades, research on miRNAs have highlighted that their fine mechanism of post transcriptional regulation is fundamental in almost all cellular processes. They are present not only in tissues, but also in biological fluids, as a result of active and passive releasing from different cells. These characteristics made miRNAs both good potential biomarkers and therapeutics targets for many different diseases. Moreover, a growing number of evidence shows that miRNAs are deeply involved in the skeletal muscle physiological and pathological conditions, particularly in muscular dystrophies, including DM.

The aim of my PhD project is understanding the role of microRNAs dysregulation in DM1 and the development of a DM1-specific circulating miRNA signature to use as disease biomarker.

In particular, the project is focused on two main points:

-validation in a large patient cohort of a DM1 plasma signature to use as biomarkers of disease staging/severity;

-investigating the dysregulation of miRNAs association to RISC complex in muscle biopsies derived from DM1 patients.

III. MATERIALS AND METHODS

Patients' selection and samples collection

This study was authorized by the Institutional Ethics Committees and was conducted according to the principles expressed in the Declaration of Helsinki, the institutional regulation and Italian laws and guidelines. All blood samples and skeletal muscle biopsies were taken after specific written informed consent.

Clinical diagnosis of DM1 and DM2 patients was based upon International Consortium for Myotonic Dystrophies guidelines [6] and genetic analysis was carried out to confirm DM1 [113] and DM2 diagnosis [56].

Stage of disease was determined using Muscular Impairment Rating Scale (MIRS) [114] 1 = no muscular impairment, 2 = minimal signs, 3 = distal weakness, 4 = mild–moderate proximal weakness, 5 = severe proximal weakness. Five-point MRC scale (Medical Research Council) in the upper and lower limbs for a total maximum score of 150 (MRC megascore) was used to evaluate muscle strength [115]. Specifically, the score was obtained measuring on both sides 7 muscle groups of the upper limbs (shoulder abductors and adductors, elbow flexors and extensors, wrist flexors and extensors, finger flexors) and 7 muscle groups of the lower limbs (hip flexors and extensors, knee flexors and extensors, ankle dorsiflexors and plantar flexors, extensor hallucis) as well as neck flexors and extensors. Myotonia was evaluated qualitatively during neurological examination and confirmed by needle electromyography.

Blood samples were obtained by venous punctures of 103 DM1 and 111 age and sex matched patients dysplaing no clinical signs of neuromuscular disorders (CTR) (Table 1). Moreover, 30 DM2 patients and 30 age and sex matched controls were also considered (Table 1). EDTA-tubes were used for samples preparation. Cell- and platelet-free plasma was prepared following a 2 step centrifugation protocol: samples were centrifuged at 1.500 g for 15′ at 4 °C. Next, the supernatant was centrifuged again at 14.000 g for 15′ at 4 °C and stored at −80 °C [108].

Biceps brachii biopsies of 10 DM1 patients and 10 age and sex matched healthy subjects, were harvested under sterile conditions and snap-frozen in liquid nitrogen (DM1: 3 males, 7 female, 49.0±1.9 years; CTR: 5 male, 5 female, 48.9±2.2 years).

Plasma RNA extraction

Total RNA from plasma was extracted using NucleoSpin miRNA Plasma (Macherey-Nagel) as previously described [108]. Pellets were re-suspended in 50 µl of RNAse-free water and samples were spiked-in with 25 fM of exogenous cel-miR-39 (Ambion) to assess the efficiency of RNA extraction, because Nanodrop (Thermo Scientific) quantification was not reliable, due to the low amount of extracted material.

Hemolysis was tested measuring plasma absorbance at 570 and 600 nm wavelengths, where oxy-, deoxy- and carboxy-hemoglobin display similar absorbance [116].

Plasma miRNAs quantification and scores calculation

RNA was retro-transcribed by Taqman microRNA RT kit (Life technologies), following manufacturer's instructions, and miRNAs were measured by qPCR using TaqMan microRNA assays (Life technologies), performed in duplicate. Relative expression was calculated using the comparative Ct method [117]. To calculate ΔCts values, the average of 3 normalizers was used: spike in cel-miR-39 and 2 endogenous stable miRNAs, miR-106a and miR-17-5p, as previously described [108]. Next, to calculate ΔΔCt values, DM1 and individual controls were all compared to a reference pool of all control RNAs (control mix), measured in quadruplicate, ensuring comparable results throughout the study.

For the scores calculation, ΔΔCt values were converted to a linear scale, using the formula $2^{\wedge(-\Delta\Delta Ct)}$ to represent the up-regulations, while for the down-modulation, data were calculated as $-2^{\wedge(\Delta\Delta Ct)}$.

Subsequently, "DM1-miRNA score" was obtained by averaging the fold changes for all validated miRNAs, while for "myomiR score" and "miR-133a/b score", the average of miR-1,-133a, -133b,-206 or only miR-133a and -133b were used, respectively.

Ago2 immunoprecipitation in skeletal muscle tissue and RNA extraction

- *Lysate preparation*

Biceps brachii biopsies were homogenized by Tissue Lyser (Quiagen) in RIP lysis buffer of Magna RIP™ RNA-binding protein Immunoprecipitation kit (Merck-Millipore, Billerica, MA, USA). In particular, 100 µl of complete lysis buffer was prepared for each sample, mixing 97 µl of RIP lysis

buffer, 0.5 µl of Protease cocktail inhibitor and 0.25 µl of RNAse inhibitor (Merck-Millipore). After homogenization and protein quantification, lysed samples were snap frozen in liquid nitrogen and stored at -80°C until use.

- *Preparation of magnetic beads*

To prepare the magnetic beads, 50µl of beads suspension was used for each sample and washed twice with 0.5 ml of RIP wash buffer, placing the tubes on a magnetic separator (MagnaRck™, Invitrogen). After the second washing, 5 µg of RIPAb+ Ago2, Monoclonal Anti-Ago2 (11A9,Sigma Aldrich) or Normal mouse IgG (Merck-Millipore) were added, in order to precipitate Ago2 protein or aspecific negative control for each homogenized sample, respectively. The beads were incubated with the antibodies for 30 min at room temperature (RT) on a TubeRotator (VWR®). After the incubation, the beads were separated on the magnetic rack and washed twice with 0.5 ml RIP wash buffer.

- *Immunoprecipitation*

A RIP immunoprecipitation buffer was prepared for each sample, mixing 860 µl of RIP wash buffer with 35 µl of 0.5M EDTA and 5 µl of RNAse inhibitor (Merck-Millipore).

In each tube containing Ab-conjugated beads, the wash buffer was replaced by 900 µl of RIP immunoprecipitation buffer and frozen lysate was rapidly thawed and centrifuged ad 14.000 rpm for 10 minutes at 4°C. After this step, 50 µg of lysate was used to extract "input RNA" and mixed with 200µl of TRIzol® reagent (Invitrogen™), while the remaining material was divided in half between Ago2 and negative control assays. All the tubes were then incubated with rotation for 4 hours at 4°C, and then, the tubes were placed on the magnetic separator to perform five washes, with 0.5 ml of RIP wash buffer. After the last washing, the beads were separated on the magnetic rack, the supernatant discarded and 200µl of TRIzol® (Invitrogen™) was added to each sample.

- *RNA extraction*

Input and immunopurified (IP) samples harvested in TRIzol®, were let at RT for 2-3 minutes, then, after the addition of chloroform (40µl), were vortexed and centrifuged at 12000xg, at 4°C for 15 minutes. Next, the aqueous phases were transferred into clean tubes, and 5µg of Glycogen (Roche) and 104µl of Isopropanol (SigmaAldrich) were added to each sample. Afterward, the RNAs were let to precipitate at 4°C up to 2 hours and then centrifuged at 12000xg for 10 minutes at 4°C.

Pellets were washed two times with 1 ml of 80% ethanol (Sigma-Aldrich), centrifuged at 5000xg for 5 minutes at 4°C and, after the last washing, pellets were let to dry and finally re-suspended in 10-15

µl of sterile water. In the samples to be processed for small RNAs sequencing, a spike in control small RNA (cel-miR-39, 25 fMol) was added during the extraction procedure to be used for normalization.

Protein quantification

The protein quantification was performed using the Pierce™ BCA Protein Assay kit (Thermo Scientific), which is based on bicinchoninic acid (BCA) for the colorimetric detection and quantitation of total proteins. Standard curves were prepared using diluted albumin (BSA, 2mg/ml) standards and the absorbance at 562nm was measured by Victor^3 Multilabel Plate Reader (PerkinElmer).

RNA sequencing and gene ontology (GO) analysis

RNA-Sequencing was used to measure small and long RNAs deriving from RISC-IP samples, while for total RNA, only small RNAs were sequenced. All total RNAs were checked for integrity (RIN) by Bioanalyzer (Agilent) according to manufacturer's instructions, while RNAs derived from IPs were impossible and to check for integrity, given the very low amount of material. Previous experiments indicated that 50-100 ng RNA/skeletal muscle biopsy were recovered

RNA sequencing was performed in collaboration with Dr. Jose M. Garcia-Manteiga (Center for Translational Genomics and Bioinformatics, S. Raffaele Institute, Milan-Italy), by Illumina next generation sequencing (NGS) platform HiSeq 2000. The RNA-seq of small RNAs included barcoded and pooling of samples in 4 pools containing both IP small RNAs and total small RNAs. Small RNA libraries were prepared using the TruSeq Small RNA Sample Preparation Kit (Illumina). The cDNA was then PCR amplified using specifically designed primers. This protocol takes advantage of the natural structure common to most known mature miRNAs having a 5'-phosphate and a 3'-hydroxyl group as a result of enzymatic cleavage by Dicer or other RNA processing. Because of this, the RNA adapters are ligated to each end of the RNA molecule and an RT reaction is used to create single stranded cDNA.

mRNA libraries were generated with Ovation RNA-Seq System V2 (NuGen) which allows to prepare amplified cDNA starting from small total RNA amounts. Amplification was initiated at the 3' end as well as randomly throughout the whole transcriptome in the sample, allowing the amplification of both mRNA and non polyadenylated transcripts.

After trimming of sequencing adapters (trimmomatic), the sequences quality was checked with FastQC (http://www.bioinformatics.babraham.ac.uk/projects/fastqc/). The alignment to the genome (hg19) was made with BWA (Burrows-Wheeler Aligner) [118] and the counting of features was made with htseq-count (v0.5.3p9) against the mirbase 19 annotation.

Linear Models for Microarray Analysis (LIMMA) with the voom function [119] were used to find differentially overrepresented miRNAs in RISC samples of DM1 patients vs controls. In parallel, long RNAs differentially present in RISC IP complex of DM1 vs Healthy patients were identified using LIMMA/voom. In order to find miRNAs predicted targets, miRtrail software was used (http://mirtrail.bioinf.uni-sb.de/upload.php).

The gene ontology analysis was performed using WebGestalt (http://www.webgestalt.org) software, considering only mRNAs with a stastically significant differential expression between the two groups.

RNA sequencing validation by qPCR

Input and IP RNAs were retro-transcribed with Taqman microRNA RT kit (Life technologies) and Ovation qPCR system (Nugen) to obtain cDNA for miRNAs and mRNAs expression, respectively. For miRNAs RT, 10 ng of input RNA and 0.5 µl of IP RNA were retro-transcribed on Thermal Cyclers (Bio-Rad), using Taqman microRNA specific assays.

The cDNA amplification was performed by Taqman Fast 2x PCR Master Mix (Life technologies) on Applied biosystems 7900HT Fast Real-time PCR system or on StepOne Plus Real-time PCR system (Thermo Fisher Scientific). For mRNAs RT, 20 ng of input RNA and 2 µl of IP RNA were used. The cDNA amplification was performed by SybR Green Master Mix (Life technologies) and genes specific primers (Table 1).

The oligos were designed using Integrative Genomics viewer (IGV) [120], UCSC Genome Browser (http://genome.ucsc.edu) and Primer-BLAST (https://www.ncbi.nlm.nih.gov/tools/primer-blast). All qPCR measurements were performed in triplicate, and miR-181a and RPL23 were used as housekeeping genes for miRNAs and mRNAs validation, respectively.

Table 1. Primer sequences used for RNA-sequencing validation.

GENE NAME	PRIMER FORWARD	PRIMER REVERSE
ACTC1	TCTGTCCACCTTCCAGCAAA	TGAGGGAAGGTGGTTTGGAA
ASB2	TGGGCCACGTCTTCATCTTA	AAACCTCTATTCCTGGGGCC
COL21A1	CCTGTTGTTCGGTGTTGTGA	AGGCATACAACAAACATTCCGA
ERBB3	ATGTCCATTATGCCCGCCTA	ACCTGGGAGAGAGAGGGAAT
FST	GCTGTGCCCTGACAGTAAGT	GTAGCACACCTGAGGAGCAG
MYBPH	TCAAACTCCAGAGATGCCCA	CCCTTGAGCCCAGTTAGTCT
RPL23	TCCGGATTTCCTTGGGTCTT	TGTTCAGCCGTCCCTTGATC
SESN3	CCTTCAGCACCGTACACCTA	GTGGCTGGTGATGTTTGGTT
WEE	TGCCTTGTGAATTTGCTGCT	AGGAGGGAAAGGGTGCATTT

Cells culture, myotubes differentiation and characterization

Immortalized fibroblasts derived from adult patients (DM1, CTR,) were obtained in collaboration with Dr. Germana Falcone laboratory (National Research Council, Rome-Italy). The cell lines were inducible for MyoD under the control of estrogen receptor. The growing medium was constituted by DMEM High glucose (Gibco), 15% Fetal Bovine Serum (FBS, Euroclone), L-Glutamin 200x (Sigma-Aldrich), Penicillin-Streptomycin 100x (Sigma-Aldrich) and Puromycin (0.2 µg/ml, Serva Electrophoresis). The differentiation medium was prepared DMEM high glucose without phenol red (Gibco), 2% horse serum (Sigma-Aldrich), Insulin (10µg, NovoMix), Estradiol ($10^{\wedge -4}$ M, Sigma Aldrich) and Penicillin-Streptomycin 100x (Sigma-Aldrich) was used.

Cells were grown on 0.5% gelatin (Bio-Rad) and, when 90% of confluency was reached, the growing medium was replaced by the differentiation one. After 4 days in the differentiation medium, cells have been lysed by home-made lysis buffer: 150mM KCl (Sigma-Aldrich), 25 mM TrisHCl (Sigma-Aldrich) pH 7.4, 5 mM EDTA (Sigma-Aldrich), 0.5% NP40 (Sigma-Aldrich), 5 mM DTT (Sigma-Aldrich), 1 mM PMSF (Sigma-Aldrich), Protease Inhibitor Cocktail Kit (100x, Thermo Scientific), RNAsin (0.2 U/µl, Merck-Millipore). After lysis, the protocol of Ago2 immunoprecipitation was performed, using Pierce™ Protein A/G Magnetic beads (ThermoFisher Scientific) and 5 µg of RIPAb+ Ago2 or Normal mouse IgG (Merck-Millipore) used as described above.

Fluorescent in situ hybridization (FISH) with MBNL1 co-localization, in myotubes coltures

All reagents used were RNAse free, prepared with distilled water Diethylpyrocarbonate (DEPC) treated. Cells were fixed in 2% paraphormaldehyde for 30 min at 4°C. After 5 washings with PBS 1x (Gibco) at RT, they were permeabilized by Triton 0.4% in PBS (Gibco) for 5 minutes at RT.

Then, cells were incubated in the pre-hybridization buffer (40% Formamide and SSC 2x, Sigma Aldrich)) for 10 minutes at RT, and then in the hybridization buffer: 40% formamide (Sigma-Aldrich), SSC 2x (Sigma-Aldrich), 0.02% BSA (Sigma-Aldrich), 67 ng/µl tRNA, 2mM Vanadyl ribonuclease complex, 1 ng/µl $[CAG]_6$ probe and DEPC H_2O for 2 hours at 37°C in a humid chamber.

Next, the cells were washed in post-hybridization buffer (40% formamide and SSC 2x) for 30 min at 65°C, then 3 washes were performed in: SSC 2x for 15 min at 65°C, SSC 1x for 15 min at 65°C and SSC 1x for 10 min at RT. Then, cells were incubate with NGS (Normal Goat Serum, Dako) diluted 1:20 in PBS+2%BSA, for 20 minutes at RT. Subsequently, an overnight incubation with the antibody anti-Mbnl1 (1:1000 in PBS +2% BSA, provided by Prof. C.A. Thornton, University of Rochester) was performed; then, an anti-rabbit AlexaFluo 488 (1:400 in PBS+2% BSA) was used for 1 hour at RT (1:400 in PBS+2%BSA). After 3 washing in PBS 1x for 5 minutes, cells have been incubated with DAPI (1:1000 in SSC 20x) for 30 min at RT. Finally, after 5 washing in PBS, samples were prepared using Mowiol mounting medium.

Statistics

Continuous variables are expressed as mean ± standard error (SE) unless indicated differently. The box plots represent data divided in quartiles. For group-wise comparisons, Mann–Whitney U test was used. The ability to discriminate between the DM1 and control groups was determined by the receiver operating characteristic curve, and the area under the curve was calculated. A ROC curve allows to visualize the reciprocal relationship between sensitivity (true positive fraction) and specificity (false positive fraction) and is an effective method to evaluate the performance of diagnostic tests. The calculation of sensitivity and specificity depends on the threshold value used to separate the two classes. As the thresholds gets higher, specificity increases and sensitivity decreases; conversely, lower threshold levels correspond to decreased specificity and increased sensitivity. [121] The Area Under Curve (AUC) is a value of diagnostic accuracy that quantifies the overall ability of the test to discriminate between control and diseased individuals. It ranges from totally non-informative (AUC = 0.5) to perfect test (AUC = 1) [122,123].

Spearman rank correlation was used to compare miRNA levels with clinical characteristics. For multiple linear regression, absolute ΔΔCt were used to study the association between all the scores and clinical characteristics. The normality of the scores was assessed through histogram visualization. Outliers were identified by Tukey's test. All tests were performed 2-sided and $p \leq 0.05$ was considered as statistically significant, except for RNA-sequencing, where results showing a False Discovery Rate (FDR) ≤ 0.1 were considered. For statistical analysis GraphPad Prism v. 7.0 (GraphPad Software Inc.) and R (R Core Team (2013)) software were used, unless differently indicated.

IV. RESULTS

IV.I. CIRCULATING miRNAs AS POTENTIAL DM BIOMARKERS

Plasma miRNA validation in DM1 patients

Platelet-free plasma samples were harvested from 103 DM1, and 111 age- and sex- matched control (CTR) patients, displaying no neuromuscular disorders. DM1 patients presented the typical hallmarks of myotonic dystrophy, summarized in table 2 [50]. Most of the patients were in stage 3 of the disease (MIRS score) [114] and the pathological CTG expansions ranged from 65 to 1400.

Of note, there was no overlap between the patients and controls analyzed in this study and the ones analyzed in our previous investigation [108]. Total RNA was extracted from plasma samples and miRNAs were measured by qPCR.

For this validation study, we measured miR-133a, miR-193b, miR-191, miR-140-3p, miR-27b, miR-454, miR-574, miR-885-5p and miR-886-3p, previously described in Perfetti et al. [108], and miR-1, miR-206 and miR-133b identified by Koutsoulidou and collaborators [107].

Normalization is a critical issue in all circulating miRNA studies [125]. For this reason, three normalizers were used, one exogenous (cel-miR-39) and two endogenous (miR-106a and miR-17-5p). The high number of DM1 patients and of miRNAs tested required several qPCR sessions. To make sure to have comparable results, we used a reference sample obtained by pooling a fraction of all control preparations. Given that normalization is a fundamental step in this kind of studies, and in order to obtain maximum specificity, were considered as validated only those miRNAs that displayed significant differences after normalization with all the following normalizer combinations: 1) the average of cel-miR-39, miR-106a and miR-17-5p (Figure 3); 2) exogenous cel-miR-39 only (Figure 4a); 3) the average of the two endogenous miRNAs, miR-106a and miR-17-5p (Figure 4b). In this way, it was confirmed that in DM1, 8 miRNAs out of 12 were deregulated.

Particularly, miR-27b was the only one down-modulated, while miR-133a,-133b,-140-3p, -454 and-574 were up-regulated. It is worth noting that values obtained with all normalization criteria were very similar, confirming data robustness.

Table 2. Clinical characteristics of DM1, DM2 and control patients recruited for blood samplings.

CLINICAL CHARACTERISTICS	DM1, n=103	DM2, n=30	CTR, n=111
Age at sampling (average ± se)	44.1 ± 1.3	54.7 ± 2.7	43.0±1.0
Age of onset (average ± se)	25.9 ± 1.3	41.5 ± 2.4	NR
Sex (male/female)	58/45	13/17	51/60
MRC megascore (average ± se)	118.6 ± 1.9	143.5 ± 1.4	150.0±0.0
Myotonia (% of patients)	87	54	0
Glucose (normal values: 70-110 mg/dl)	88.7 ± 1.2	112.3 ± 13.6	90.3±1.3
Cholesterol (normal values: <200 mg/dl)	212.0 ± 6.7	230.1± 9.6	204.0±6.0
CK (normal values: male<190 mg/dl, female <125 mg/dl)	Male: 280±3.5	Male: 313.9±86.6	Male: 128.8±27.2
	Female: 224.6 ±22.7	Female: 353.6.6 ±95.0	Female: 124.5±24.1
Arrhythmia (% of patients)	38	12	0
Cataract (% of patients)	56	32	0
ECG-QRS duration (normal values: 60-110 ms)	103.5±4.3	99.1±4.5	NA
Number of CTG repeats (range)	484.0 ± 27.6 (65-1400)	NA	NA
Stage of disease (range 1-5) (% of patients at each stage)	Stage 1: 5	NR	NR
	Stage 2: 29	NR	
	Stage 3: 34	NR	
	Stage 4: 28	NR	
	Stage 5: 3	NR	

NA: not available; NR: not relevant

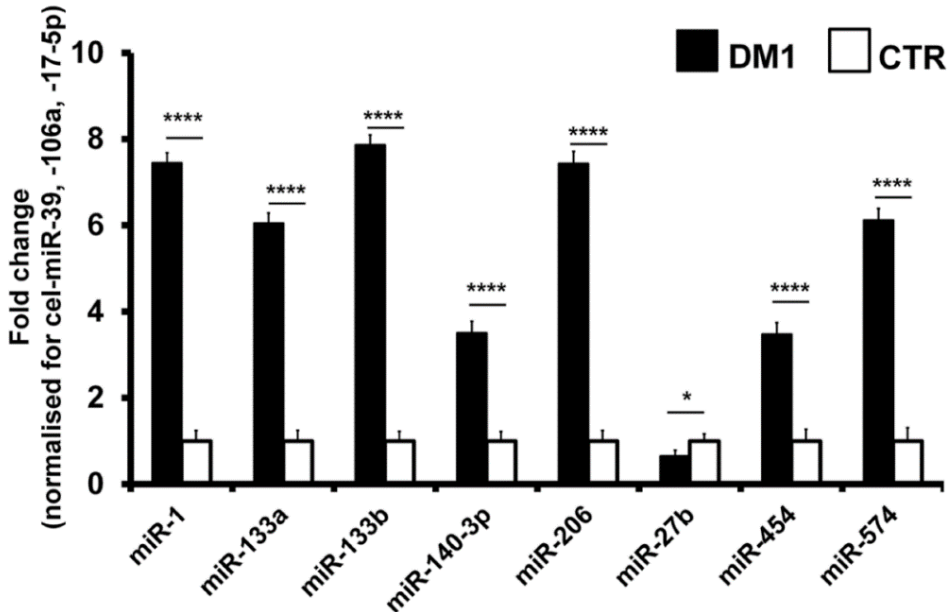

Figure 3 Validation of plasma miRNAs in DM1 patients using all 3 normalizers. The bar graph represents mean values of the indicated miRNAs in plasma of DM1 patients compared to controls (CTR). Average values of cel-miR-39, miR106a and 17-5p were used for normalization (DM1 n=103, CTR n= 111; **** p<0.0001, * p<0.05).

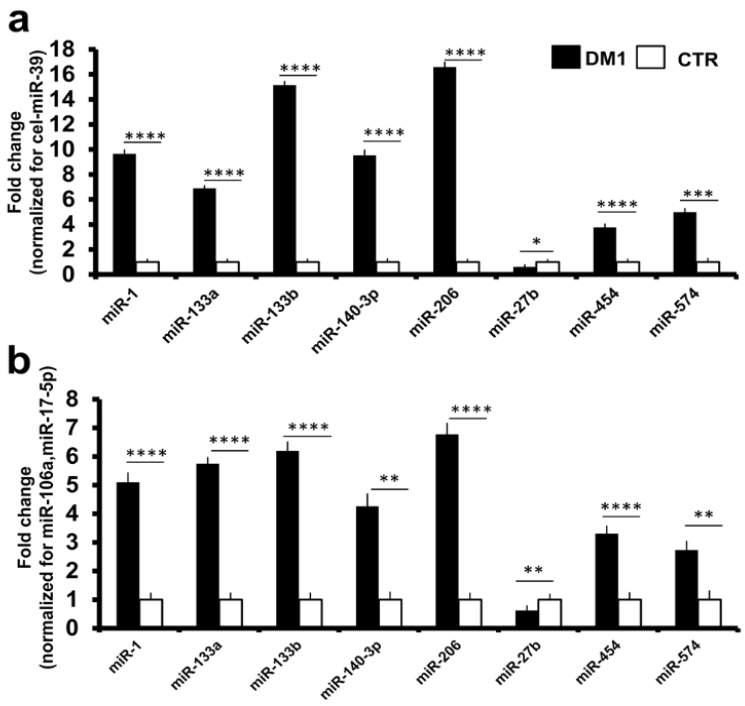

Figure 4 Plasma signature with different normalization criteria. The bar graphs represent the significantly modulated miRNAs using different combinations of the 3 normalizers comparing DM1 versus CTR patients. (DM1 n=103, CTR n=111; **** p<0.0001, *** p<0.001, ** p<0.01, * p<0.05). a) Average values of cel-miR-39 were used

Deregulated plasma miRNA signature accurately identify DM1 patients

To test the accuracy of deregulated miRNAs, Receiver Operator Characteristics (ROC) curves were calculated for each plasma miRNA found differentially expressed in DM1. In this way, it was found that miR-133b (table 3) displayed the highest Area Under Curve (AUC=0.82), and all myomiRs exhibited similar AUCs (from 0.79 to 0.81, table 3). Non-myogenic miRNAs, instead, presented lower but still significant values (from 0.58 to 0.81, table 3).

Table 3. Area under curves (AUC) of each validated plasma miRNAs in DM1 compared to controls.

microRNA	AUC	Confidence Interval (C.I.)	p-value
miR-133b	0.82	0.76-0.87	<0.0001
miR-1	0.81	0.74-0.86	<0.0001
miR-133a	0.80	0.74-0.86	<0.0001
miR-206	0.79	0.73-0.85	<0.0001
miR-574	0.71	0.63-0.68	<0.0001
miR-454	0.70	0.62-0.76	<0.0001
miR-140-3p	0.69	0.61-0.76	<0.0001
miR-27b	0.58	0.50-0.66	<0.05

In order to test whether combining the values of different miRNAs, allowed even better performances, three scores were calculated. The first, named "DM1-miRNA score", was obtained averaging the fold changes obtained from all miRNAs, as described also in [108] (Figure 5); the second is the "myomiRs score", obtained averaging the fold changes of myomiRs only (i.e. miR-1, -133a, -133b and miR-206) (Figure 6). The last one, miR-133a/b score, was obtained averaging the fold changes of miR-133a and b (Figure 7). As shown in table 3 all scores present AUCs better than miR-133b alone, with AUC of 0.85 for DM1-miRNA score (Figure 5), 0.87 for the myomiR score (Figure 6) and 0.86 for miR-133a/b score (Figure 7).

In particular, considering a cut-off value of 2.55, sensitivities of 81.6%, 82.3%, and 82.5% as well as specificities of 70.3%, 71.2% and 71.2% were observed for the DM1-miRNAs score, the myomiR score and the miR-133a/b score, respectively.

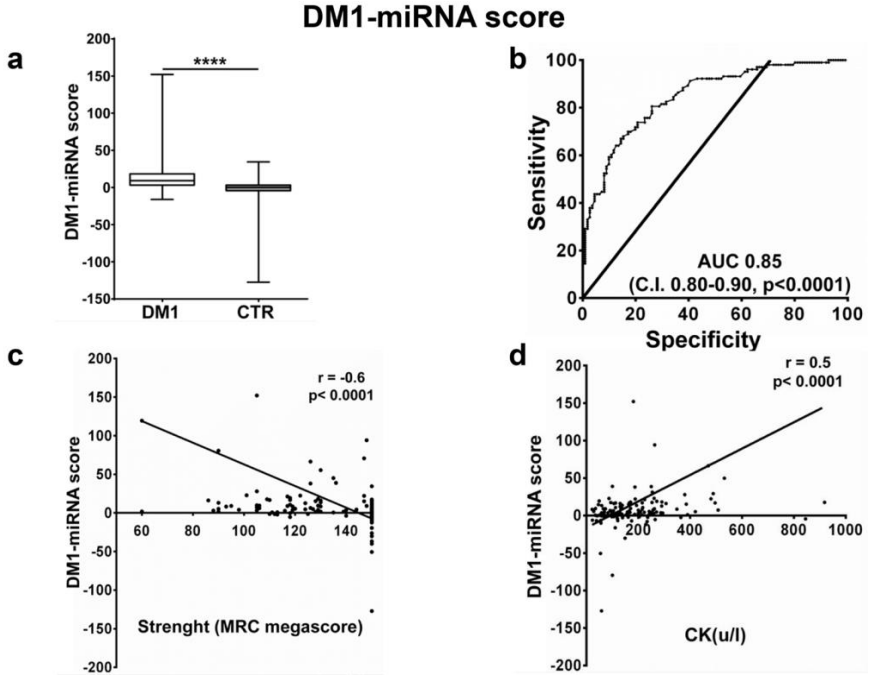

Figure 5. DM1-miRNA score validation as DM1 biomarker. The DM1-miRNA score was calculated averaging the fold changes of miR-1, -133a, -133b, -140-3p, -206, -27b, -454 and -574 in the plasma of DM1 and controls (DM1 n=103, CTR n=111). a) Box plot of DM1-miRNA score levels in the plasma of DM1 and controls (CTR; **** p<0.0001). b) ROC curve illustrating sensitivity and specificity of the DM1-miRNA score in discriminating healthy from diseased patients. c) Spearman's inverse correlation between the DM1-miRNA score and muscle strength measured by MRC megascore. d) Spearman's direct correlation between the DM1-miRNA score and CK plasma levels.

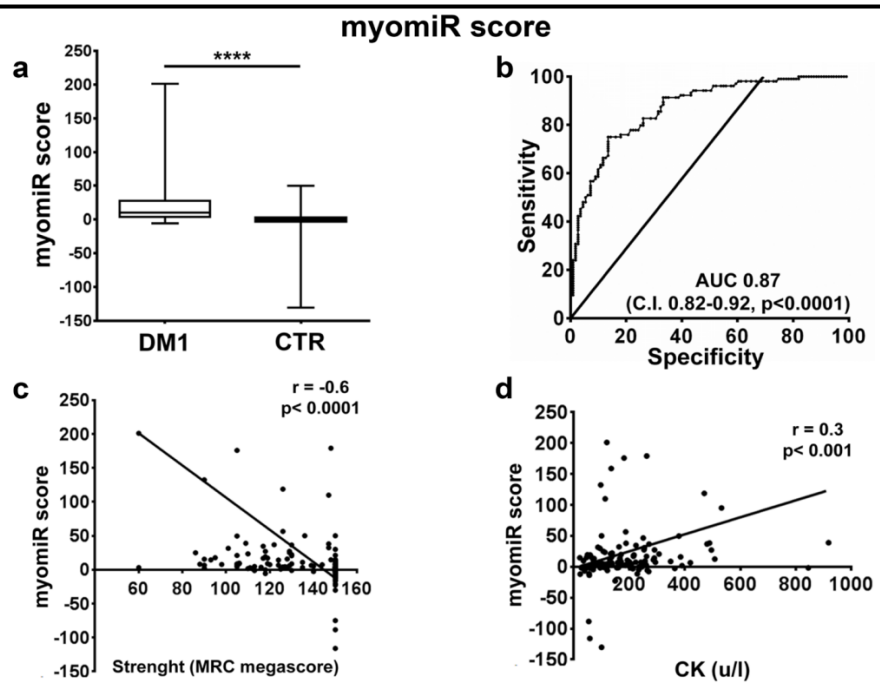

Figure 6. myomiR score validation as DM1 biomarker. The myomiR score was calculated averaging the fold changes of miR-1, -133a, -133b, and -206 in the plasma of DM1 and controls (DM1 n=103, CTR n=111). A) Box plot of myomiR score levels in the plasma of DM1 and controls (CTR; **** p<0.0001). B) ROC curve illustrating sensitivity and specificity of the myomiR score in discriminating healthy from diseased patients. C) Spearman's inverse correlation between the myomiR score and muscle strength measured by MRC megascore. D) Spearman's direct correlation between the myomiR score and CK plasma levels

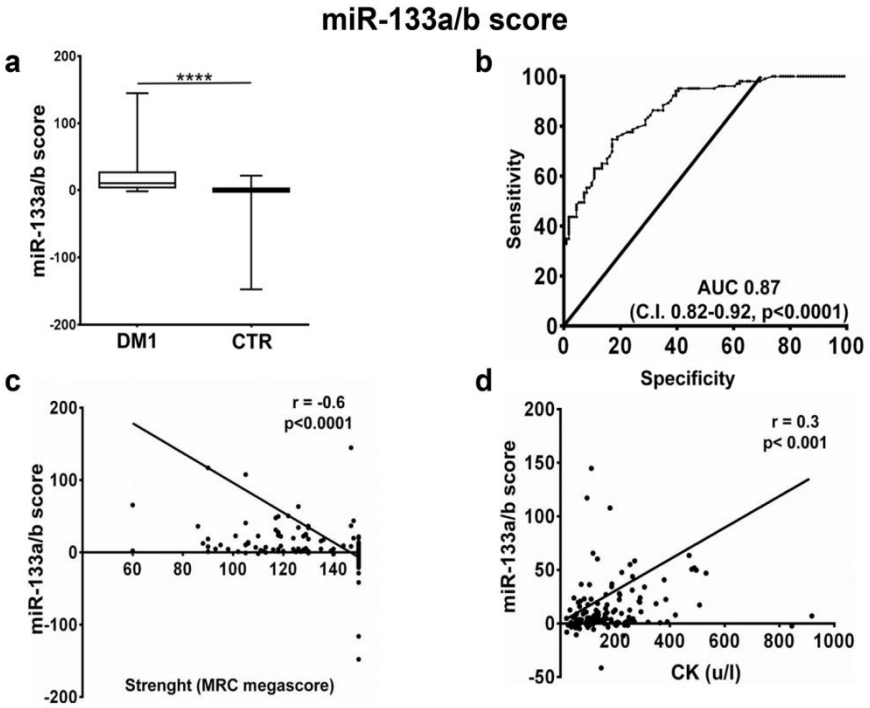

Figure 7. miR-133 a/b score validation as DM1 biomarker. The miR-133a/b score was calculated averaging the fold changes of miRNA-133a and -133b in the plasma of DM1 and controls (DM1 n=103, CTR n=111). A) Box plot of miR-133a/b score levels in the plasma of DM1 and controls (CTR; **** p<0.0001). B) ROC curve illustrating sensitivity and specificity of the miR-133a/b score in discriminating healthy from diseased patients. C) Spearman's inverse correlation between the miR-133a/b score and muscle strength measured by MRC megascore. D) Spearman's direct correlation between the miR-133a/b score and CK plasma levels

Finally, we also found that, using different normalization procedures, similar AUC values were obtained for all scores, confirming the robustness of the data (Table 3).

Table 5. Are under curves (AUC) obtained with different normalization criteria

	Data normalized vs				
	Average (miR-106a, -17, -39)	**miR-39**	**miR-106a**	**miR-17**	**Average (miR-106a, -17)**
All miRs	0.85 (C.I. 0.80-0.90)	0.79 (C.I. 0.72-0.85)	0.76 (C.I. 0.69-0.82)	0.73 (C.I. 0.66-0.80)	0.76 (C.I. 0.70-0.83)
miR-133a/b	0.86 (C.I. 0.82-0.91)	0.83 (C.I. 0.78-0.89)	0.79 (C.I. 0.72-0.85)	0.77 (C.I. 0.71-0.84)	0.82 (C.I. 0.77-0.88)
myomiRs	0.87 (C.I. 0.82-0.92)	0.83 (C.I. 0.78-0.89)	0.80 (C.I. 0.74-0.86)	0.78 (C.I. 0.71-0.84)	0.81 (C.I. 0.76-0.87)

All results have p-value<0.0001.

DM1-deregulated miRNAs are similarly modulated in DM2 patients

In order to assess whether the miRNA deregulation found in DM1 patients was also observed in DM2 patients, the plasma of 30 DM2 patients (Table 2) and 30 age and sex matched control subjects was assayed. Figure 8 shows that, with the exception of miR-27b, all the other miRNAs were significantly increased, further confirming the similarity of the two DM diseases.

Next, the differentiating value of the identified miRNAs were tested in DM2 patients, calculating the same scores as for DM1, keeping out miR-27b. It was found that all three scores efficiently differentiated DM2 patients from controls (Figure 9).

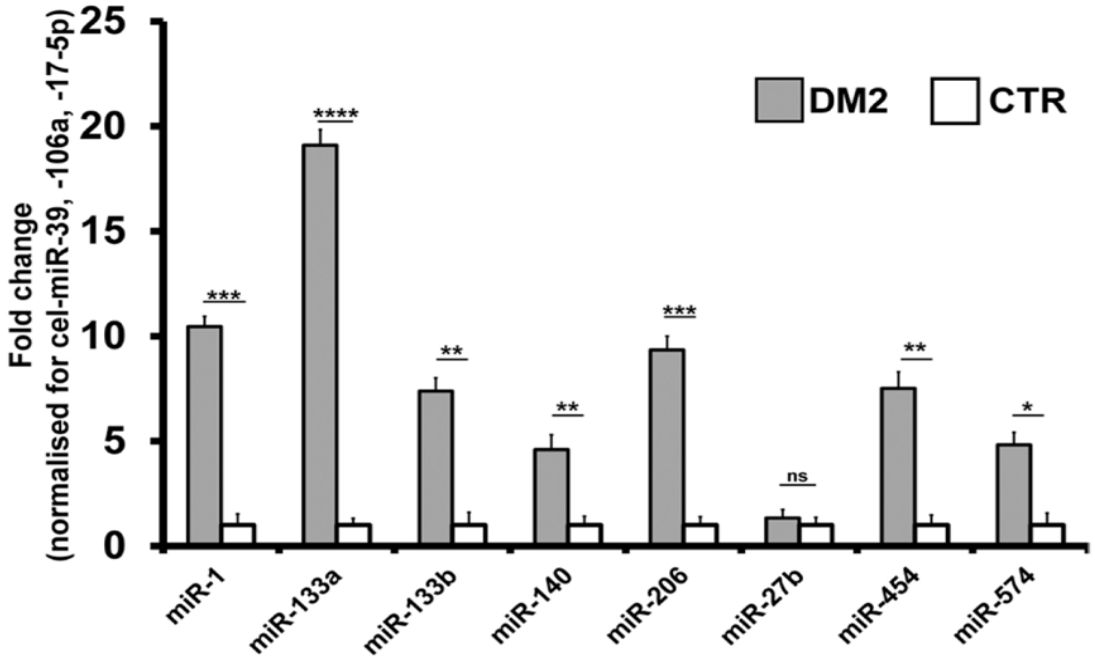

Figure 8. Validation of plasma miRNAs in DM2. The bar graph represents mean values of the indicated miRNAs in plasma of DM2 patients compared to controls (CTR). Average values of cel-miR-39, miR106a and 17-5p were used for normalization (**** $p<0.0001$, *** $p<0.001$, ** $p<0.01$,* $p<0.05$).

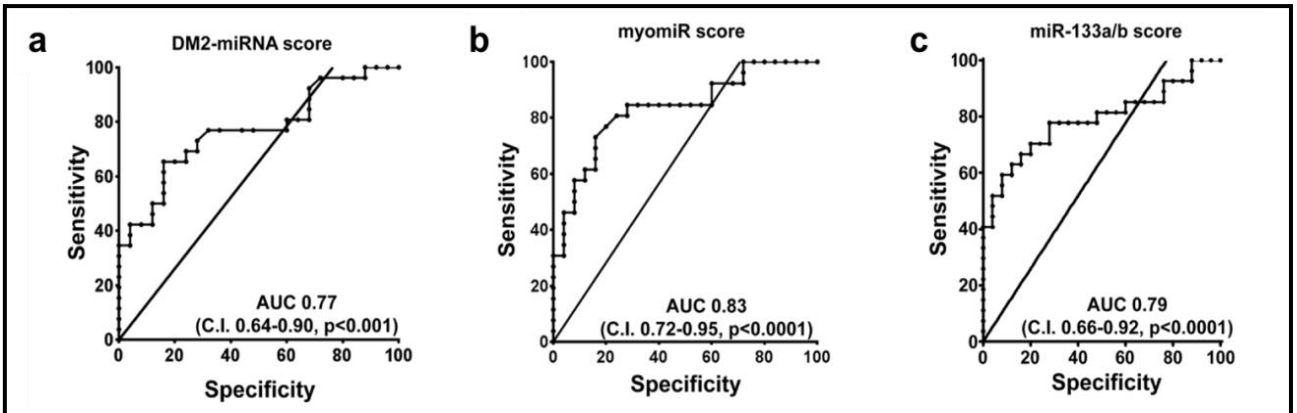

Figure 9. **ROC curves of DM2 compared to healthy subjects.** Specificity and sensibility of a) DM2-miRNA score, myomiR score (b) and miR-133a/b score (c) (DM2, n=30; CTR, n=30).

Plasma miRNAs correlation with clinical relevant parameters

Taking the results of deregulated plasma miRNAs, correlations with interesting clinical parameters have been found. Particularly, analyzing all subjects, miR-133b levels (Figure 10a) and all three scores displayed a weak, but still significant correlation with muscle strength (MRC, figures 5, 6 and 7 c) and a correlation with CK levels (Figures 5, 6 and 7 d and figure 10 b). One of possible limitation of the latter result is that exercise in the days before testing was not recorded.

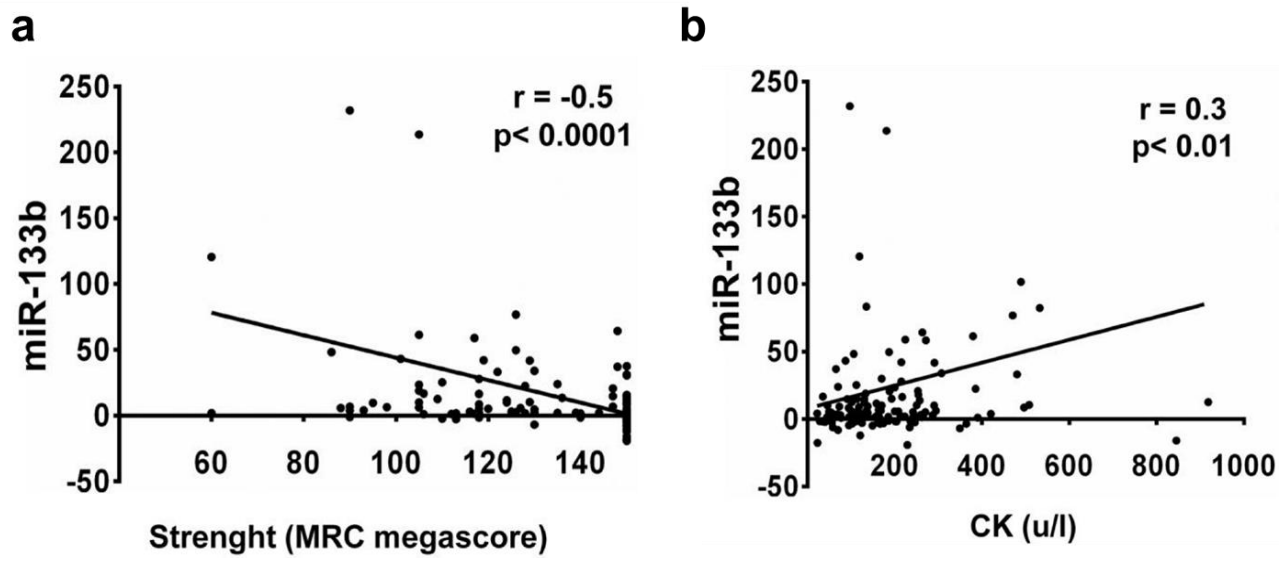

Figure 10. Correlation between miR-133b and some clinical parameters. A) Spearman's inverse correlation between miR-133b fold changes and skeletal muscle strength and B) direct correlation with plasma levels of creatine kinase (DM1, n=103, CTR, n=111).

Moreover, we also found that miR-133b levels were significantly higher in female DM1 patients compared to DM1 males, while no difference was observed in control subjects (Figure 11). This difference was present with all three normalization procedures.

Next, to better investigate the relationship between clinically relevant variables in DM1 patients that were most affected by disease, i.e. with MIRS >2, a multiple linear regression was performed analyzing CK values, age of onset, number of triplet expansions and muscle strength. Statistically significant associations are reported in table 6. We identified the association of muscle strength with miR-133b levels and all three scores. Moreover, CK values were associated to myomiR-score and miR-133a/b score. We can conclude that all the identified scores display good combinations of sensitivity, specificity and correlation with clinically relevant features.

Considering the minimization of the number of assays as an important parameter for the transferability to the clinical practice, also a miR-133a/b score obtained using only the two internal normalizers (Table 5) displayed features very similar to these obtained using the three normalizers (Figure 7b).

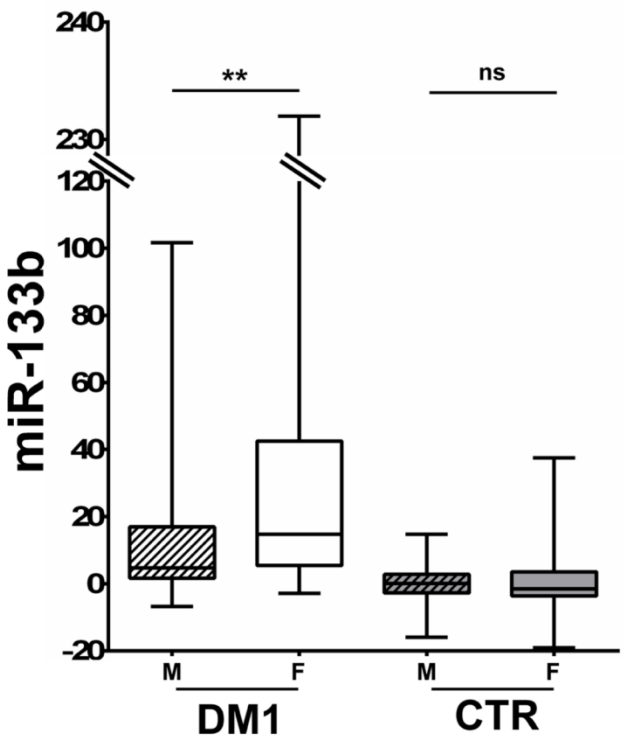

Figure 11. miR-133b plasma levels are higher in DM1 female population. Box and whiskers represents minimum and maximum values (DM1, n=103, CTR, n=111, ** $p<0.01$, ns = not statistically significant).

Table 6. Multiple regression analysis, DM1 patients with stage of disease higher than 2

SCORE	PARAMETERS	COEFFICIENT	STD ERROR	p-value
DM1-miRNA	ΔMRC[a]	0.036	0.013	0.011
myomiR	ΔMRC	0.042	0.015	0.007
	CK	0.004	0.002	0.033
miR133a/b	ΔMRC	0.038	0.014	0.011
miR-133b	ΔMRC	0.059	0.019	0.005
	CK	0.005	0.002	0.035

IV.II. EXPRESSION PROFILING OF RISC-ASSOCIATED SMALL RNAs AND mRNAs IN SKELETAL MUSCLE BIOPSIES FROM DM1 PATIENTS

Experimental design

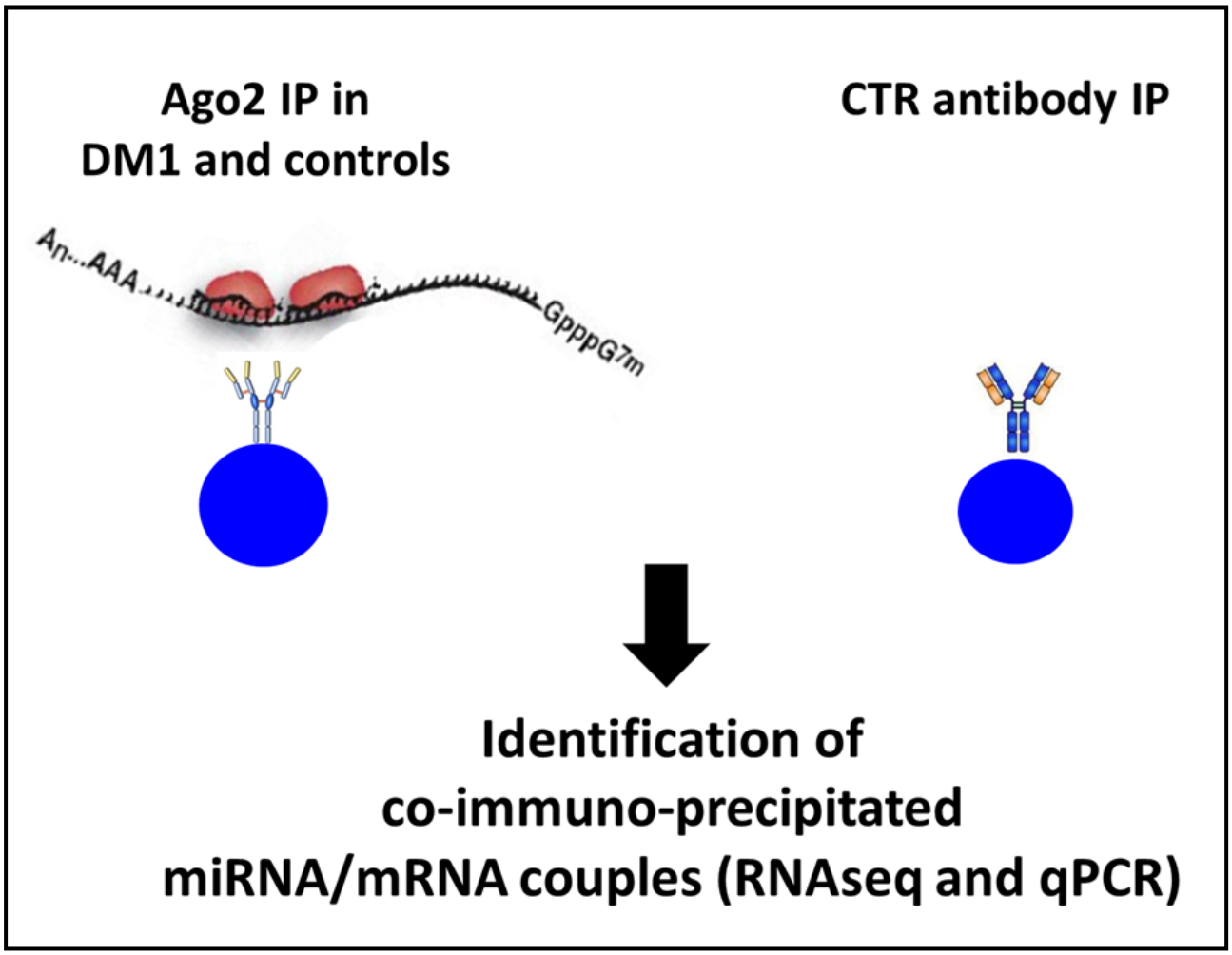

Setting up of the experimental conditions

Conditions for Ago2 immunoprecipitations had been set up in the past by our group [97], but in cells of mouse origin. In order to set up the Ago2 immunoprecipitation protocol in human muscle biopsies, tissue lysates were immunoprecipitated with two Ago2 antibodies, and analyzed for miRNA co-precipitation. miR-1 and miR-221 were readily detectable in immunoprecipitates obtained with both Ago2 antibodies(Figure 13a). Next, mRNAs enrichment was also tested in Millipore RISC-IP samples. Figure 13 b shows that indeed both, p27 and GAPDH mRNAs were easily detectable in

Ago2 immunoprecipitates (Figure 12 b). Thus, Millipore Ago2 antibody was used in all RISC-IP experiments.

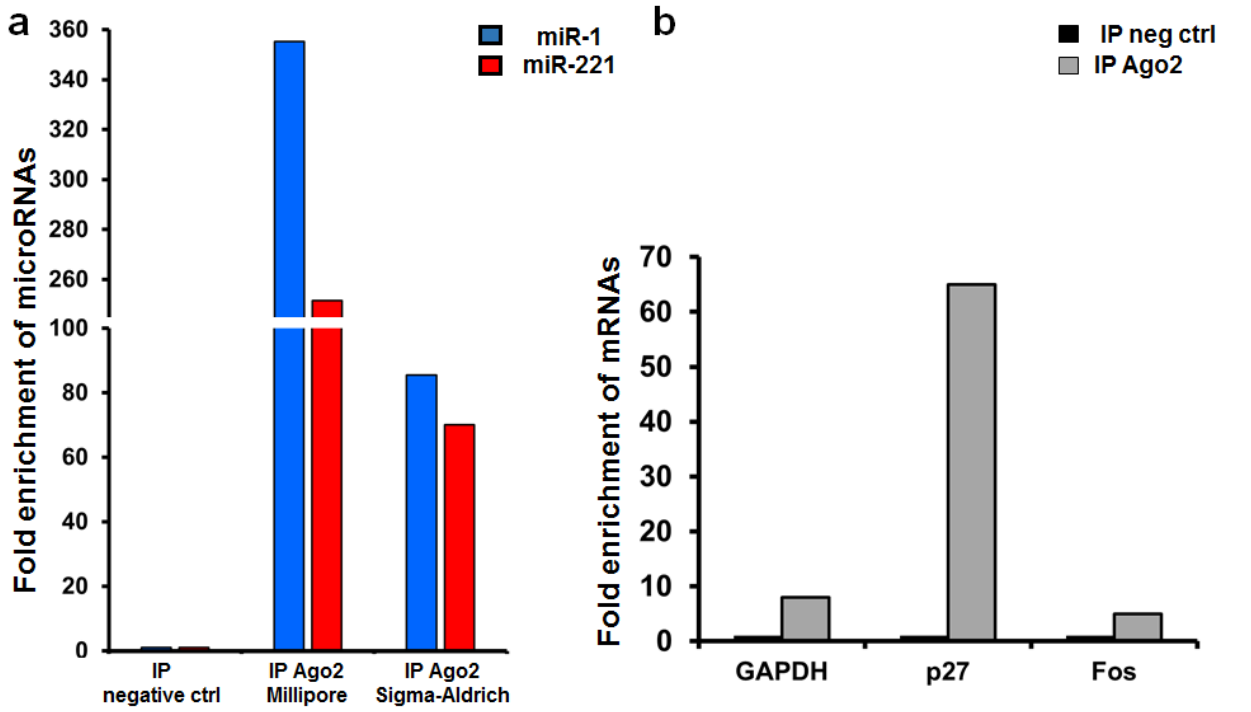

Figure 12. Enrichment of miRNAs and mRNAs in RISC-IP immunoprecipitations. The tissue lysate derived from one skeletal muscle biopsy was mmunoprecipitated by Millipore or Sigma antibodies and separated by magnetic beads. Next, the co-immunoprecipitated RNAs were extracted and analyzed by qPCR a) The levels of miR-1 and miR-221 were normalized against U6 RNA. b) Specific enrichment of p27, GAPDH, and c-Fos mRNAs in Ago2 Millipore IP, normalized for U6 RNA levels. In both graphs, fold enrichment was calculated against the negative control, referred as 1.

RNA sequencing pilot experiment

RNA derived from immunoprecipitated samples is very low abundant (50-100 ng/sample), and RNA-sequencing conditions from low RNA amounts had already been set up for long RNAs, but not for small RNAs (miRNAs). Thus, a pilot small RNA sequencing experiment was performed, using either 1 µg of total RNA, as indicated by manufacturer's instructions, or 50 ng. For this pilot experiment, total RNA was derived from skeletal muscle biopsies of one control and one DM1 patient.

Using an adapted protocol consisting in a higher number of PCR cycles, thus producing more abundant small RNA bands, we managed to produce good quality libraries. The sequencing of these

libraries yielded very similar results in terms of small RNAs identified and quantified to what obtained with the recommended amount of starting material (1 µg) (Figure 13).

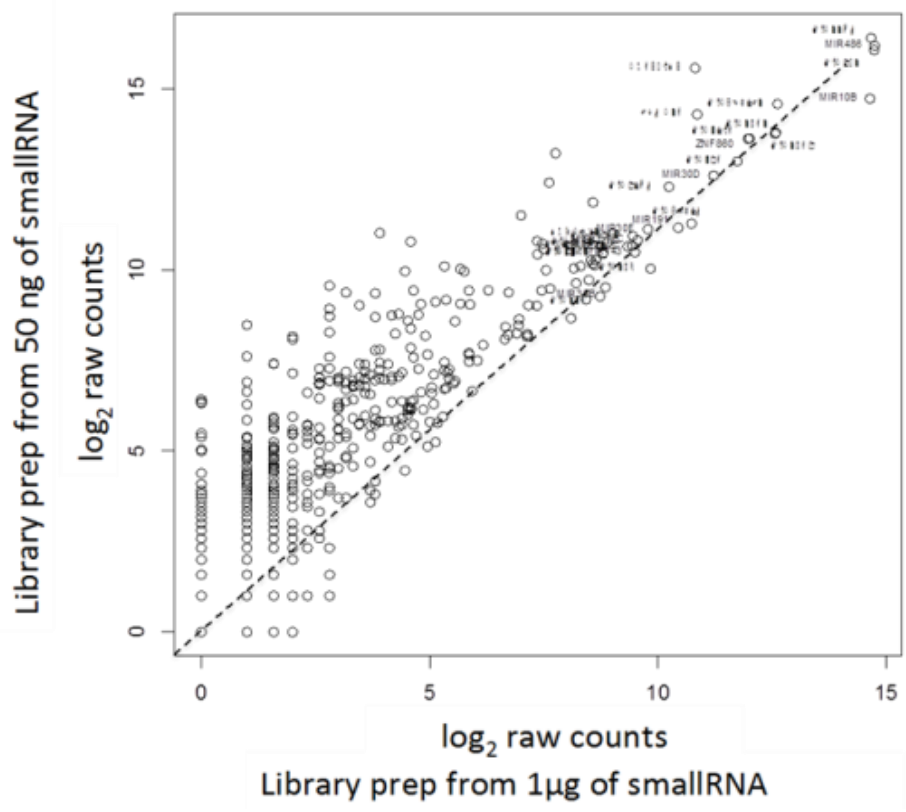

Figure 13. Setting the small RNAs library preparation protocol. Libraries prepared from 50 ng and from 1µg of RNA yielded similar results. Low represented small RNA were amplified at higher levels using 50 ng likely reflecting the effects of a higher number of PCR cycles. The reads mapping to medium and high abundance small RNAs were well correlated in the two preparations.

Then, it was concluded that 50 ng of RNA were sufficient to perform small RNA sequencing.

RNA sequencing of small RNAs and mRNAs in DM1 patients.

Duplicate biopsies from biceps muscles of 3 healthy individuals and 3 DM1 patients were used to extract either total (Input) RNA or RNA derived from RISC-IPs. The RNAs quality control was performed with Input samples, using Bioanalyzer, which confirmed that all RIN values were > 7.

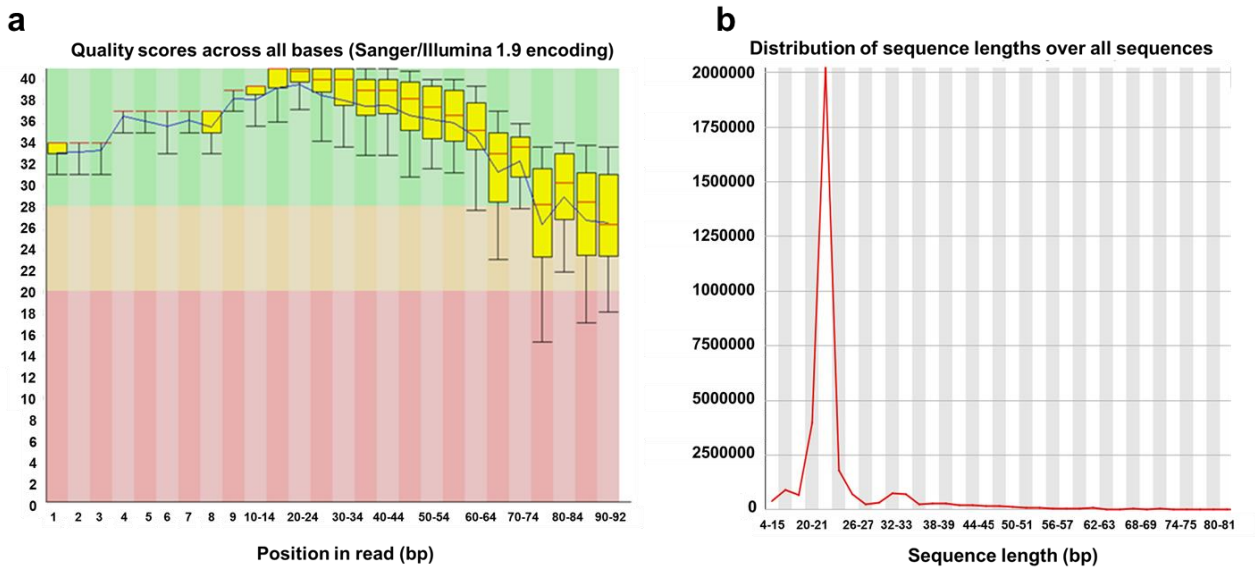

Figure 14. Quality control of smallRNA sequencing libraries. After trimming of the adapters, sequences displayed good quality (a) and a size distribution (b) showing enrichment in microRNAs (21-22 bp) and piRNAs (32 bp).

RNA sequencing results displayed high quality and the expected distribution of mRNAs and small RNAs reads (Figure 14)

Moreover, the principal component analysis showed the expected separation between DM1 and control samples, both for long RNAs (mRNAs) and for small RNAs (miRNAs) (Fig.15)

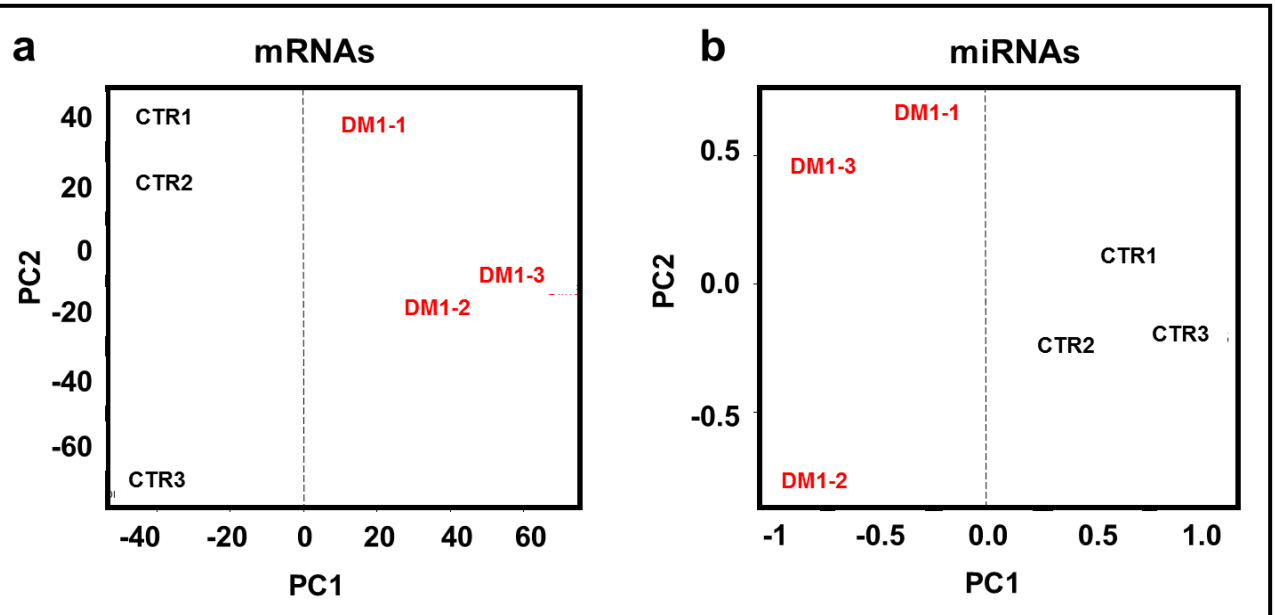

Figure 15. Principal component analysis clearly separate the two groups. Samples distribution after long RNAs (a) and small RNAs (b) sequencing.

In order to highlight differentially expressed mRNAs and miRNAs in the RISC-IP samples of DM1 compared to control patients, a False Discovery Rate (FDR) <0.1 was considered. Among 12796 mRNAs detected by sequencing, 101 genes were found significantly deregulated in DM1 RISC complexes (Figure 16), while, in miRNAs analysis, among 208 detected, 37 resulted differently represented in IPs from DM1 patients (Figure 17). Moreover, by looking at miRNA predicted targets using miRTrail [126] amongst the mRNAs and the differentially expressed miRNAs in RISC complexes, we found several miRNA-mRNA couples deregulated in DM vs healthy muscle samples (table 7). Both correlations (miRNA up and target up or viceversa) and anticorrelations (miRNA up and target down) were found. Both correlation and anticorrelation can be functionally explained, depending on the regulatory mechanisms exerted by the RISC-associated miRNAs vs their target transcripts (translational control or mRNA degradation) [72].

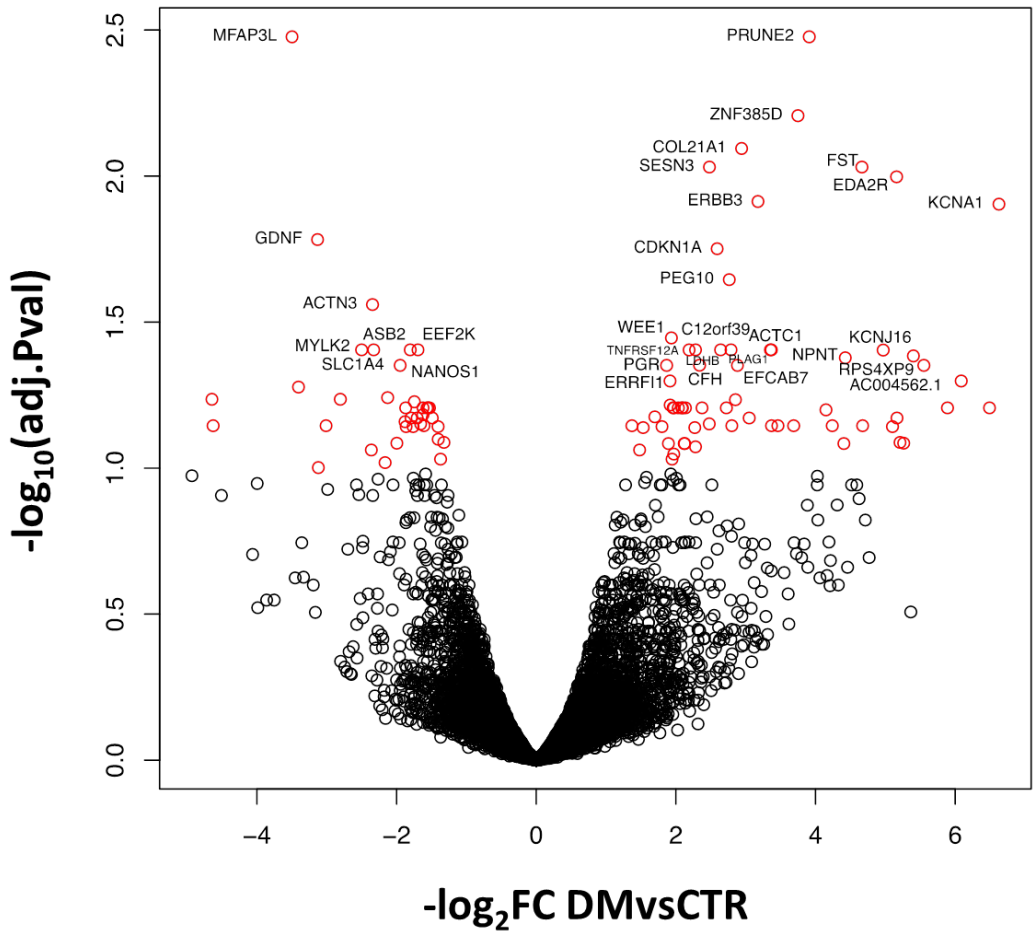

Figure 16. Volcano plot of differentially expressed mRNAs revealed by RNA-sequencing. Red dots represent statistically significant genes (FDR<0.1). (DM1, n=3; CTR, n=3).

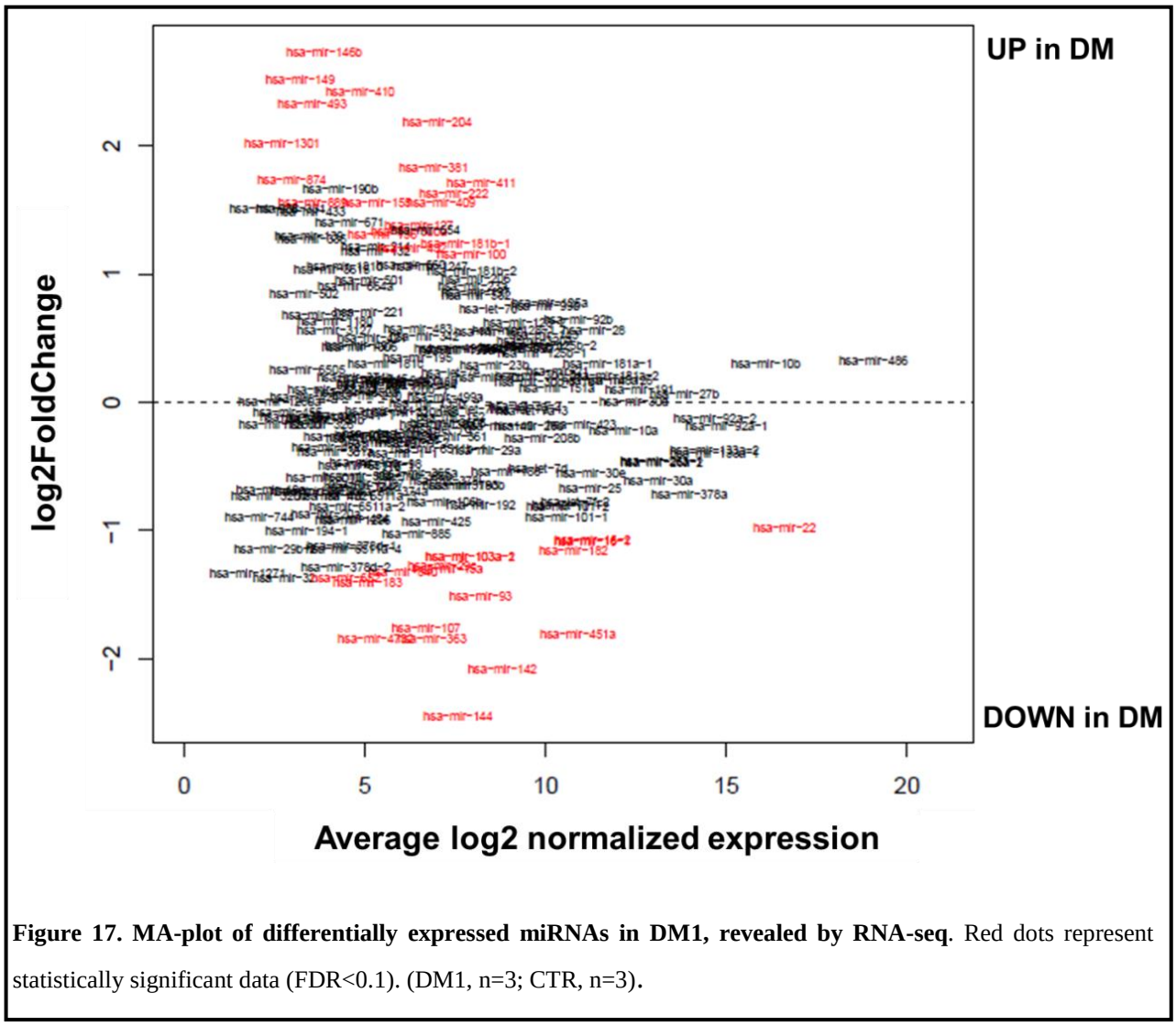

Figure 17. MA-plot of differentially expressed miRNAs in DM1, revealed by RNA-seq. Red dots represent statistically significant data (FDR<0.1). (DM1, n=3; CTR, n=3).

Table 7. DM1 RISC-enriched miRNAs associated to their differentially expressed mRNA targets.

miRNAs	Target mRNAs
miR-15a	SRPR; ACTC1; WEE1
miR-155	COL21A1; WEE1; TSPAN13; SESN3; FHOD1; LRP1B; CFH
miR-22	ERBB3
miR-29c	MYBPH; WDR47; DDAH1; CSPG4; ASB2
miR-222	TSPAN13; SLC35F1;MYLK2
miR-381	LRP1B; DUSP3; LEPREL1
miR-411	FST; GPSM2

Red and green colors indicate increased and decreased expression in DM1 RISC-IP samples compared to controls, respectively (FDR<0.1).

RNA-sequencing results showed that amongst the most abundant miRNAs present in DM1 RISC complexes we could find miR-222, miR-381, miR-146b and miR-411, previously found involved in skeletal muscle physiopathology (Greco, 2009, Greco 2012, Khanna, 2014; Harafuji, 2013); among mRNA transcripts, ERBB3 (*Erb-B2 Receptor Tyrosine Kinase 3*), FST (*Follistatin*) and ACTC1 (*Actin, Alpha, Cardiac Muscle 1*) are deeply involved in skeletal muscle metabolism [127–129].

Gene ontology analysis

Gene ontology analysis of the mRNAs dysregulated in DM1 was performed with WebGestalt software, using different enrichment analysis. KEGG analysis showed that among the top pathways represented by differentially expressed genes (FDR<0.1), there were glycolysis and gluconeogenesis (Figure 18), two important biological processes altered in DM [130].

Moreover, in the Pathways commons database, interestingly, the mRNAs dysregulated in DM1 were found enriched also in the insulin and Akt pathways, which are involved in DM pathogenesis (Figure 19) [1,131].

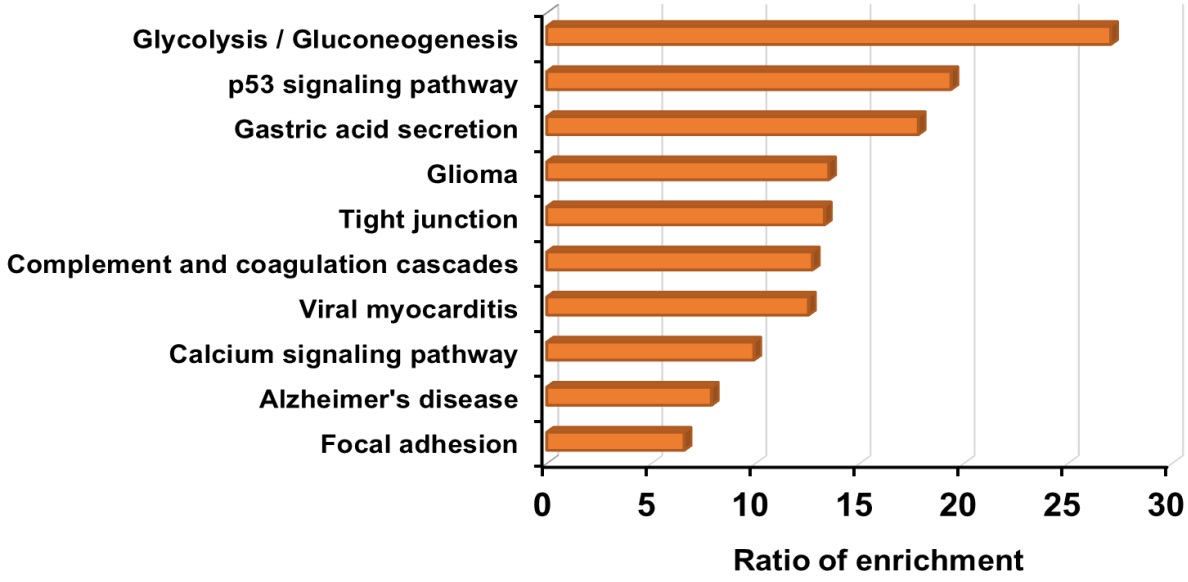

Figure 18. Enrichment analysis with KEGG pathways. Top 10 pathways enriched by differentially expressed mRNAs found in RISC complexes of DM1 compared to controls (DM1, n=3; CTR, n=3, FDR<0.1).

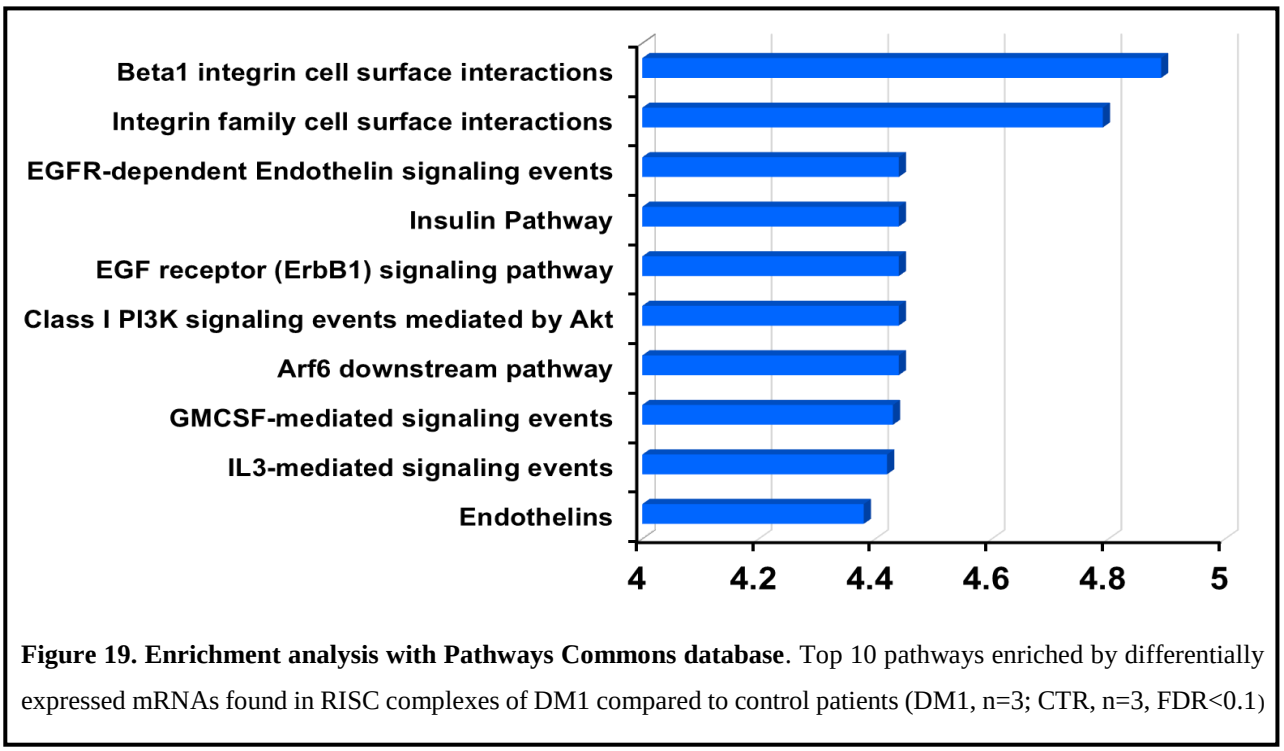

Figure 19. Enrichment analysis with Pathways Commons database. Top 10 pathways enriched by differentially expressed mRNAs found in RISC complexes of DM1 compared to control patients (DM1, n=3; CTR, n=3, FDR<0.1)

RNA sequencing validation in skeletal muscle tissue

In order to validate miRNAs and mRNAs found differentially expressed in RISC-IP samples by RNA sequencing, qPCR was used. To select the miRNAs and mRNAs to validate, the following criteria were used: regarding mRNAs, only genes that were target of differentially expressed miRNAs, presenting an FDR≤0.05 were considered; on the other hand, only those miRNAs that were significantly modulated in RISC complexes of DM1 and at the same time had modulated targets, were taken into consideration for validation analysis. In this way, 8 mRNAs and 7 miRNAs (Table 8) were selected for qPCR assays, in RISC immunoprecipitations from skeletal muscles of 8 DM1 and 8 CTRL samples.

Table 8. RNA-sequencing results about selected differentially expressed mRNAs and miRNAs in RISC-IP samples.

Modulation (DM1 vs CTR)	mRNAs	miRNAs
UP	ACTC1, FST, ERBB3, WEE, SESN3, MYBPH, COL21A1	miR-381, miR-411, miR-222, miR-155,
DOWN	ASB2	miR-22, miR-29c, miR-15a

Figure 20 shows that 6 mRNAs were confirmed to be differentially expressed in DM1 patients compared to healthy subjects. In particular, SESN3 (*Sestrin 3*), ACTC1 (*Actin, Alpha, Cardiac muscle I*), FST (*Follistatin*), WEE1 (*WEE1 G2 Checkpoint kinase*), ERBB3 (*Erb-B2 Receptor Tyrosine kinase 3*) were up-regulated (Figure 21 a, b, d, e and f) in RISC complexes of DM1 and only one, ASB2 (*Ankyrin Repeat And SOCS Box Containing 2*), down-modulated (Figure 20 c).

Moreover, these results were also analyzed in Input RNAs, confirming that their enrichment or depletion in RISC complexes was not due to a similar modulation in total RNAs (Figure 21), but rather the modulation in total RNA was often absent or in the opposite direction.

RNA-sequencing results about selected miRNAs showed that in RISC-IP samples, 4 were enriched and 3 decreased in DM1 vs healthy subjects (Table 8). In particular, miR-381, 411, -222 and -155 were found to be up-regulated in DM1, while miR-22, -29c and -15a were down modulated.

MiRNAs qPCR validation showed similar results found in RNA-sequencing, for all miRNAs. However, statistical significance was not reached in all cases, possibly due to low levels and variability among patients, miR-381 was undetectable by qPCR (Figure 21).

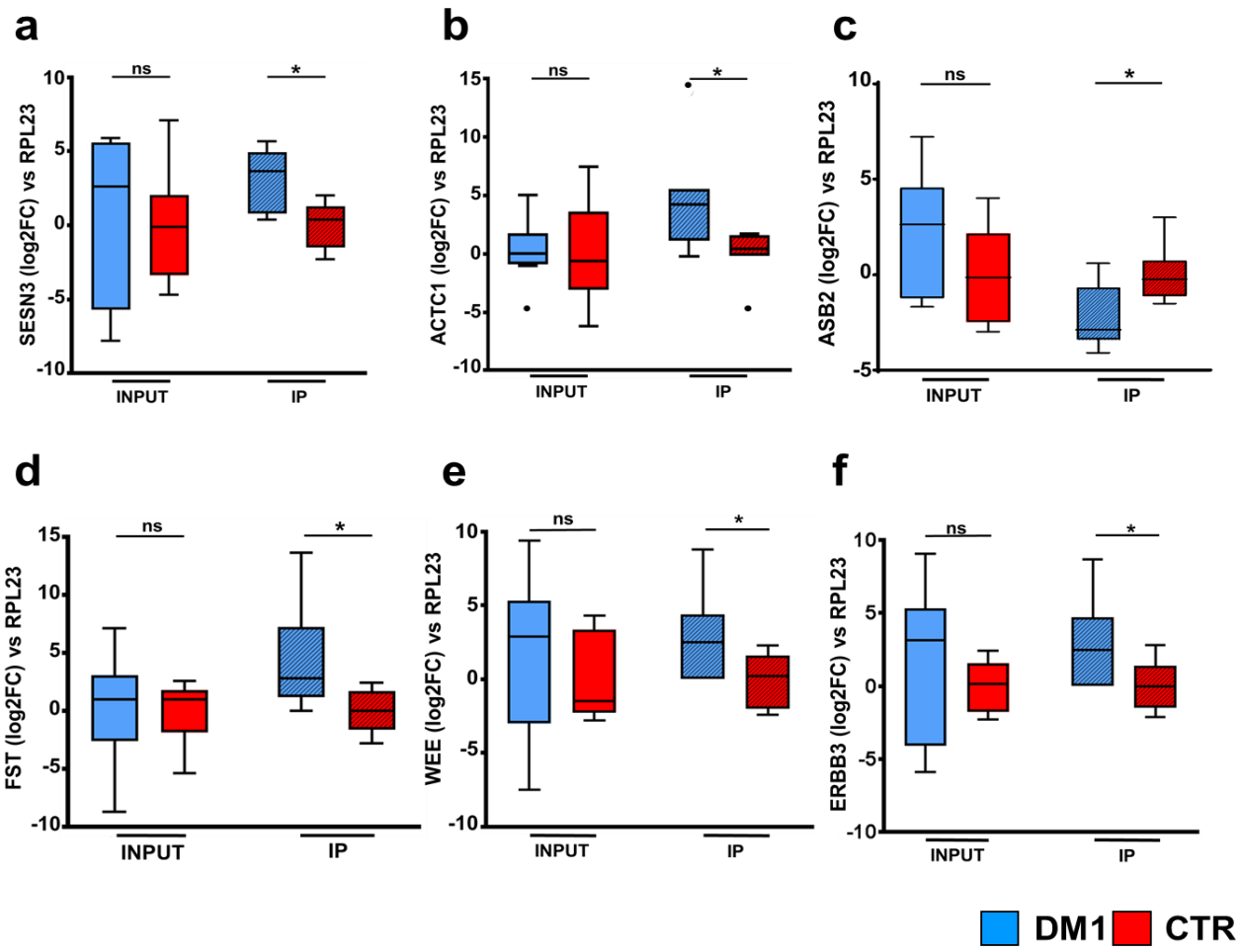

Figure 20. RNA-sequencing validation of mRNA transcripts in skeletal muscle tissue. qPCR validation of mRNA targets in DM1 vs healthy subjects. Data obtained in total (Input) RNA and RISC-IP samples are shown. SESN3 (A), ACTC1 (B), FST (D), WEE (E) AND ERBB3 (F) were enriched in IP samples of DM1, while ASB2 (C) is decreased (DM1, n=8; CTR, n=8; * $p \leq 0.05$).

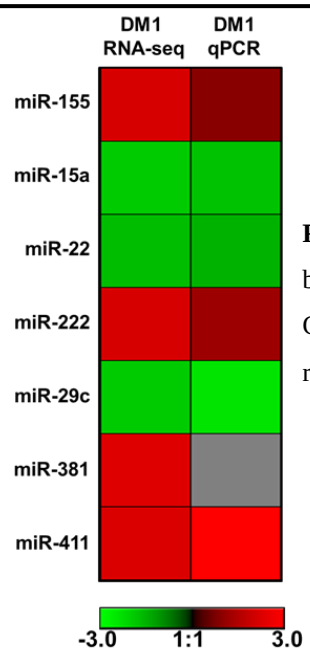

Figure 21. Heat map of miRNAs modulation in skeletal muscle tissue. Comparison between RNA-seq results (DM1, n=3; CTR, n=3) and qPCR validation (DM1, n= 7; CTR, n=6) in RISC-IP samples of DM1 compared to control subjects. Data are represented in linear scale, (ΔΔCt), referred to controls.

RNA sequencing validation in vitro

Given that the number of functional experiments that can be performed using skeletal muscle tissue is limited, we adopted a cell model of immortalized skin fibroblasts induced to differentiate into myotubes by myoD expression. For this reason, we took advantage of cells derived from adult patients, developed in close collaboration with the group of Dr. Germana Falcone (National Research Council, Monterotondo Scalo- Rome). Fibroblasts derived from DM1 patients and controls were immortalized by Telomerase expression and transduced with estrogen-inducible MyoD. After reaching the confluency (Figure 22), DM1 and CTR cells were induced to differentiate (Figure 23) and after 3 days in differentiation medium, they were treated to immunoprecipitate Ago2 protein, with a similar procedure adopted for skeletal muscles.

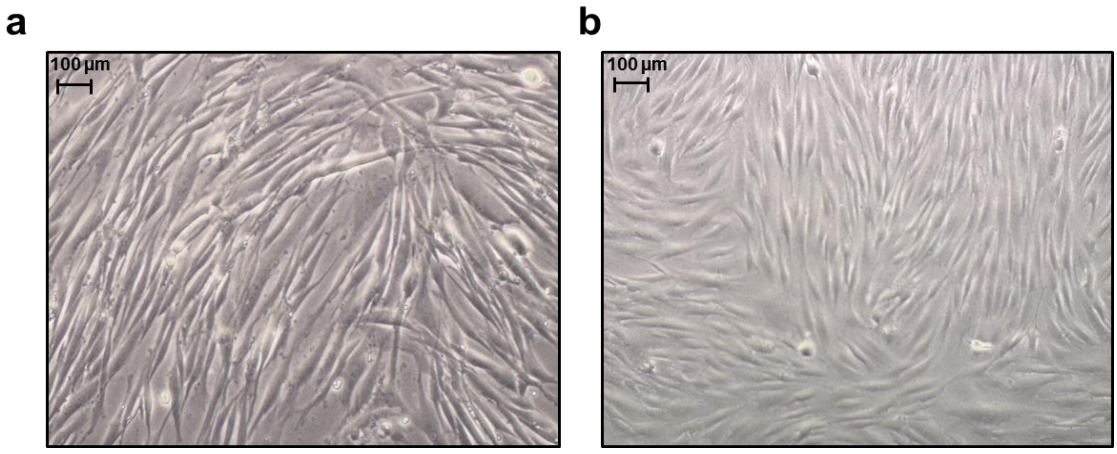

Figure 22: Immortalized fibroblasts derived from DM1 and control patients Confluent fibroblasts in control (a) and in DM1 (c) in proliferative medium (phase-contrast microscope, magnification 5X);

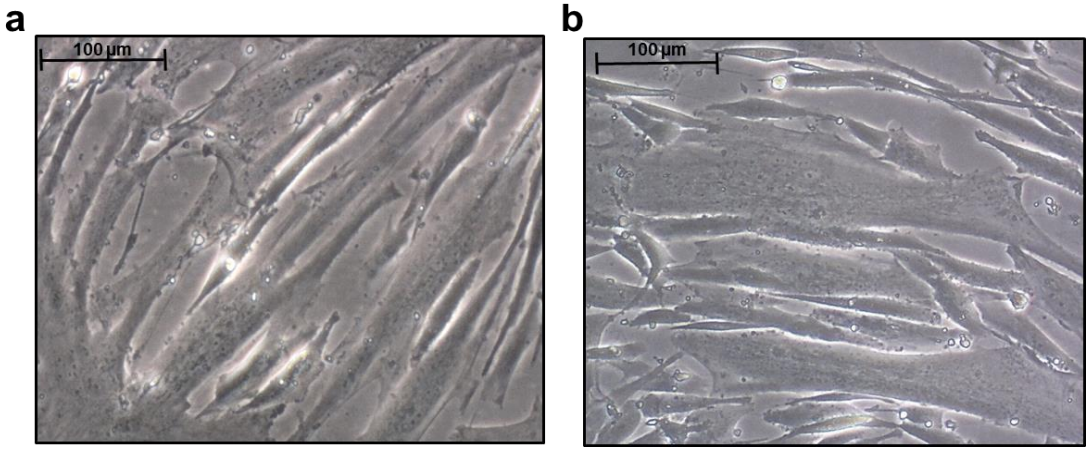

Figure 23: Immortalized fibroblasts derived from DM1 and control patients, induced to differentiate in myotubes Myotubes in control (a) and in DM1 (b) after 3 days of differentiation (phase-contrast microscope, magnification 40X).

In parallel cultures, an *in situ* hybridization was performed to verify the presence of ribonuclear inclusions (Figure 24, panels b-e) and their co-localization with MBNL1 protein (Figure 24, panels d, e and f) even after MyoD induction.

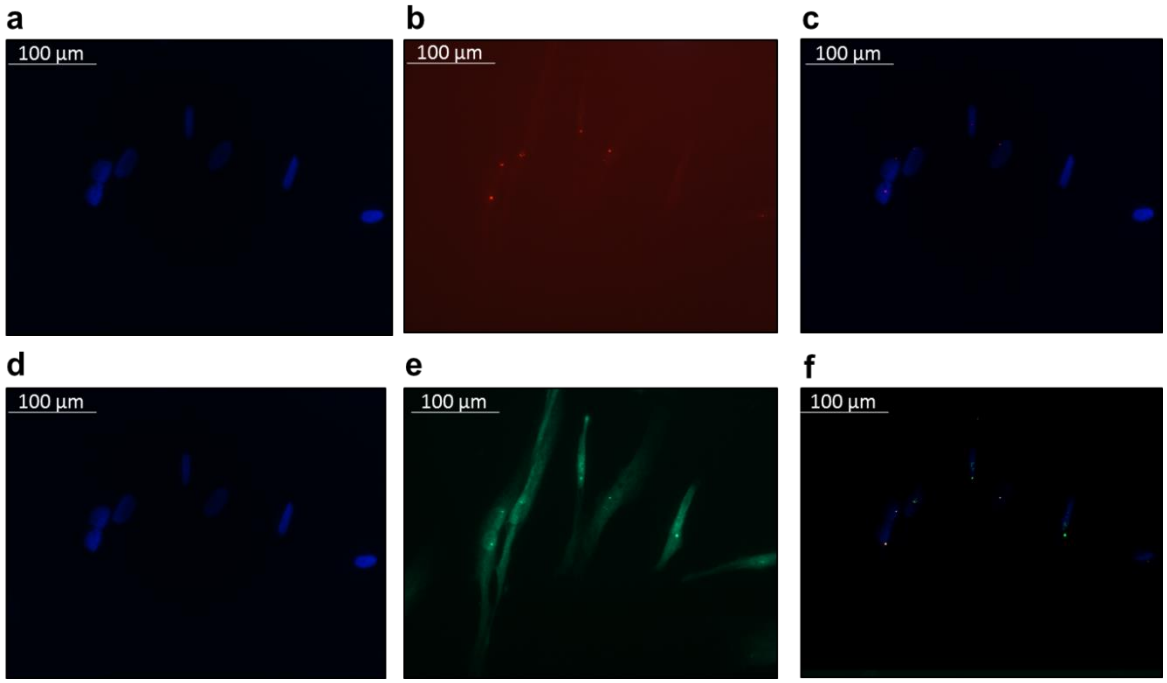

Figure 24: In situ hybridization of myotubes from DM1 patients, and co-localization with MBNL1 protein. DAPI nuclear stainings (a and d), ribonuclear inclusions (b and c) and MBNL1 localization (e and f) are represented (magnification 40x).

According to data obtained in skeletal muscle biopsies, we found that miR-411 and FST mRNA were enriched, while miR-29c and ASB mRNA were decreased in RISC-IPs of DM1 myotubes (Figure 25).

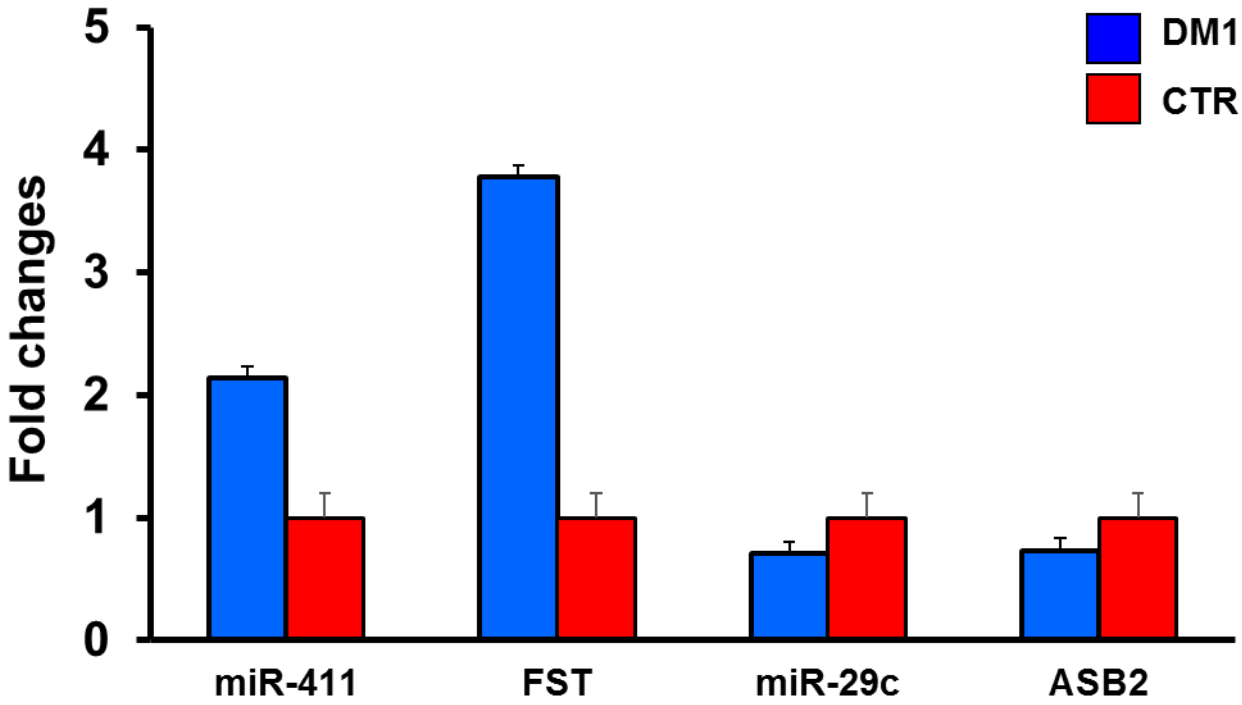

Figure 25: RISC-IP assays of cultured myotubes confirm some miRNA/mRNA couples found deregulated in DM1 skeletal muscles. RNA was isolated from RISC complexes derived from DM1 and CTR cultured myotubes. miRNAs and mRNAs were measured by qPCR. miR-411 and -29c were normalized against miR-181a, FST and ASB2 data were normalized against RPL23.

V. DISCUSSION

Although DM it is the most frequent muscular dystrophy in adulthood, the complex mechanism which gives rise to this disease is not well understood; moreover, no specific treatments are available and, to date, only the invasive method of skeletal muscle biopsy allows to accurately monitor the disease progression [5,11].

microRNAs have a fundamental role in the post-transcriptional regulation of several mRNA transcripts, associated to the protein effector complex RISC. Furthermore, they are not only present in tissues, but also in body fluids, where they are very stable and could participate to the intercellular communication or they should reflect the state of a specific organ.

Even if the research on miRNA has been booming in the last few years, miRNAs potential as therapeutic targets and as disease biomarkers in DM is still not clear. Some reports on miRNAs dysregulation in DM have been published [95,96]. However, in most circumstances, it has not been established whether these events lead to dysregulation of their miRNA targets, and to which extent. Moreover, some conflicting results are also present [95,96,132]

On the other hand, the studies about circulating miRNAs in plasma or sera of DM1 patients lack of power and of reproducibility, because of the small groups considered and the absence of a standardized normalization method [107,108].

In this study, both tissue and plasma miRNAs were studied with different approaches.

In particular, in the first part, we measured the same plasma miRNAs previously found deregulated in plasma or serum of DM1 patients in a larger and independent group, in order to corroborate or disprove the existing data. Here we analyzed more than 200 subjects between DM1 patients and controls. Albeit still limited in size, this already represents a big step forward compared to similar studies performed in rare diseases. Additionally, an accurate normalization method and stringent inclusion criteria were adopted. This approach allowed us to validate eight previously identified miRNAs, whereas four miRNAs were not confirmed, proving the importance of an accurate validation procedure. It is also worth noting that one of the RNA that were not confirmed, miR-886, is not even properly a miRNA, since it is identical to a fragment of Vault RNA 2 (VTRNA2) [133], further supporting the superior performances of miRNAs as biomarkers. Finally, it is also worth

noting that small studies also display low sensitivity. Indeed, several myomiR identified by Koutsoulidou, et al. [107] escaped identification in our previous study.

In this work, we validated the myomiR miR-1, 133a,-133b and -206 as increased in the plasma of DM1 patients. Both miR-133a/b and myomiR scores correlated, although weakly, with clinical parameters of muscle involvement, supporting the hypothesis that myomiR dysregulation in the plasma of DM1 patients is specifically related to mechanisms of muscle damage. Whether this was due to passive release from damaged myofibers, it is not known. However, unlike Duchenne muscle dystrophy, necrosis is not a DM1 disease hallmark and this increase might be due, at least in part, to active mechanisms. Interestingly, while myomiR levels are not modulated in DM1 skeletal muscle biopsies, their intracellular distribution is aberrant [96], possibly leading also to increased extracellular release.

Also interesting is the fact that miR-133b elevation was particularly prominent in DM1 female patients. While the reason for this gender difference is unknown, it is not surprising since gender is emerging as an important factor influencing DM1 clinical profile [134]. Of note, it has been found that miR-133b stimulates ovarian estradiol synthesis [135]. Whether this is related to the endocrinological abnormalities observed in DM1 patients remains to be elucidated.

Other non muscle-specific miRNAs, namely miR-140, -27b, -454 and -574 were also validated as deregulated in DM1 plasma. Indeed, since DM1 is a multisystemic disorder, it is possible that the tissue of origin of these miRNAs might not be the skeletal muscle. According to the human miRNA tissue atlas (https://ccb-web.cs.uni-saarland.de/tissueatlas), they are expressed, to different extent in multiple tissues, including brain, nerve, spinal cord, thyroid and epididymis. Thus, the plasma levels of these miRNAs may reflect the global clinical state of the patient, rather than that of a specific tissue.

Notably, the new plasma signature has also been confirmed in a small group of DM2 patients. While confirmatory studies in larger patient groups are necessary, this finding suggests that similar mechanisms underpinning miRNA release in the blood might be shared by DM1 and 2.

In skeletal muscle biopsies we have adopted an experimental strategy in order to identify both miRNAs effectively active and deregulated in DM1 patients, and their respective mRNA targets. Using a combination of RNA-sequencing, Ago2 protein immunoprecipitation, target prediction

algorithms and qPCR assays, we have found the dysregulation of very interesting miRNA/mRNA couples in DM1 patients.

The couple miR-411/FST , found enriched in RISC complex of DM1, is particularly worthy of note because both the miRNA and its target are known to be involved in the regulation of skeletal muscle mass. Indeed, miR-411 it's up-regulated in Facioscapulohumeral muscular dystrophy (FSHD) myoblasts, where it is localized in cytoplasm and regulates the suppression of myogenic factors like MyoD and Myogenin [136], affecting myogenesis. Interestingly, miR-411 increase was also confirmed in DM1 myogenic cells cultured *in vitro*.

FST is an inhibitor of TGF-β superfamily ligands, which usually repress skeletal muscle growth [128]. Overexpression of FST promotes skeletal muscle hypertrophy in primates [137], and for muscles of *mdx* mice- models of Duchenne and Becker muscular dystrophies- was found ameliorative [138]. Moreover, it has been demonstrated that administration of FST to muscles at the time of tenotomy, largely prevented the loss of muscle mass, confirming the importance of FST in the regulation of muscle integrity [128].

Given that FST is enriched in the RISC complex of DM1 patients together with its regulatory miRNA, miR-411, we should speculate that the translation of FST is much more impaired in DM1, resulting in a protein decrease, possibly contributing to the loss of muscle mass and atrophy, characterizing DM1 [1]. It is also important to underline that, on the contrary of FST, ASB2, controlled by miR-29c, is less associated to Ago2 protein in DM1 patients, and so its translation is probably more efficient in the diseased muscles. Very recently, Davey end colleagues [139] demonstrated that overexpression of FST leads to the down-regulation of *Asb2* protein, especially in young adult mouse muscles, and this is necessary for the maximal hypertrophic response to FST [139]. In the same work, it has been elucidated that expression of ASB2 resulted in a progressive muscle atrophy, indicating ASB2 as a negative regulator of basal muscle mass [139].

These findings suggest that a mechanism involving FST/ASB2 dysregulation might be involved in one of the hallmark of DM, the skeletal muscle atrophy [1]. Further studies aimed at directly testing this hypothesis are granted.

Another important miRNA which is more efficiently recruited in RISC complexes of DM1 patients is miR-222. Previous work of our group found this miRNA to be modulated during myogenesis together with miR-221, with an important role in the progression from myoblasts to myocytes and in

the reaching of a fully differentiated phenotype [140]. Moreover, very recently, our group further elucidated the role of miR-222 in myogenesis, highlighting that, repressing Rbm24 transcript, miR-222 can indirectly regulate the alternative splicing of many muscle-specific transcripts [97]. Thus, miR-222 enrichment in RISC complexes of DM1 patients is particularly intriguing, suggesting its implication in the skeletal muscle dysfunction and aberrant splicing characterizing DM1.

ERBB3 is essential in many different cell types, because it is implicated in cell growth, apoptosis and differentiation [127]. In vitro, ErbB3 along with its ligand Neuregulin, have different effects on myogenic progression. Neuregulin inhibits myogenin expression in proliferating myoblasts [141], while in myotubes promotes differentiation and muscle growth [142,143]. The fact that ERBB3 was found enriched in RISC complexes of DM1 patients, suggests its repression in diseased muscles, corroborating the hypothesis that in DM, most pathways involved in muscle mass regulation are impaired.

WEE1 is a tyrosine kinase that phosphorylates cdc25 at the G2/M checkpoint and prevents the progression to mitosis [144]. Even if its role in the skeletal muscles is not well understood, WEE1 has been found to be involved in myoblast cells death/growth arrest induced by hypoxia [145], which impairs myogenic differentiation [146,147].

ACTC1 mRNA is also increased in RISC complexes derived from muscles of DM1 patients. The multigene family of actins provides the major structural component of myofibril thin filament and both the skeletal muscle (ACTA1) and the cardiac (ACTC1) actin isoforms are expressed in skeletal muscles . [148]. Although ACTC1 is generally less abundant than ACTA1 in mature skeletal muscles, it has been found to be highly increased during muscle regeneration, characterizing activated satellite cells and regenerating myofibers [129]. Its RISC enrichment could suggests ACTC1 repression I DM1, which might be related to a reduced proliferative capacity of satellite cells, observed in DM1 [149].

Bioinformatic analysis of the pathways and functions associated to the deregulated genes also provided interesting indications. Indeed, gene ontology showed that the most represented categories were related to glucose metabolism and gluconeogenesis, which are two important pathways involved in DM pathogenesis. Indeed, in normal conditions, skeletal muscle requires an efficient glucose metabolism for its high-energy demand, in DM, the aberrant splicing of IR and pyruvate kinase M2 (PKM2) disrupts glucose homeostasis [45,130]. The fact that many genes differentially expressed in RISC complex of DM1 patients are involved in these pathways, seems to suggest that also miRNA-based mechanisms, besides the alteration of alternative splicing, might be implicated in the complex regulation of glucose metabolism.

One of the transcripts involved in glucose metabolism is SESN3, up-regulated in RISC complexes of DM1 patients. It is known that all members of Sestrins family, SESN1, 2 and 3, in humans are involved in the signal transduction through AMPK (*AMP-activated protein kinase*) and mTOR (*mammalian target of rapamycin*), which are cellular energy sensors responding to control metabolism in insulin-sensitive tissues [150]. However, it has also been discovered that SESN3 knockdown in cultured human myotubes does not impact insulin sensitivity, but increases myostatin expression, implying a role in muscle growth [150].

VI. CONCLUSIONS AND FUTURE DEVELOPMENTS

In the plasma of DM1 patients, three potentially useful miRNA scores were identified: the most simple is the miR133a/b that consists of only 2 miRNAs, facilitating the potential transfer to the clinical practice. On the other side, the DM1-miRNA score, constituted by 8 miRNAs, is more complex, but displays better correlation with clinically relevant parameters. Moreover, it is not constituted only by myomiRs, that have been found to be deregulated in other dystrophies as well [105,106]. Thus, it holds the potential to be more DM-specific. However, this remains to be determined experimentally. Also important will be a longitudinal study, to ascertain how the identified scores change over time during DM1 disease evolution.

Very important for the potential transferability to the clinics will be the development of absolute quantification assays and the identification of reference values.

As a final remark, a humoral biomarker that may facilitate disease state monitoring of the patients using a minimally invasive procedure might be particularly useful considering perspective therapeutic options, as indicated by ongoing clinical trials (NCT02312011, NCT01406873).

In the skeletal muscles we identified Ago2-associated miRNAs and mRNA targets dysregulated in DM1. These miRNA/mRNA couples seem to be mainly involved in the regulation of muscle mass and in glucose metabolism. Since muscle atrophy and insulin resistance are two main features of DM, these observations might be of potential therapeutic usefulness.

Future experiment may allow to ascertain the functional role of the identified miRNA/mRNA couples in skeletal muscle physio-pathology. To this aim, the identification of some of these miRNA/target mRNA dysregulations in DM1 myogenic cells cultured in vitro, paves the way for future functional experiments.

Also important will be assessing the relevance of the identified miRNA/mRNA couples in DM. In this respect, it will be crucial to determine how profound the impact of miRNA deregulations is on the protein levels of the relevant targets in skeletal muscles of DM1 patients.

VII. BIBLIOGRAPHY

1. Mateos-aierdi, A. J. *et al.* Muscle wasting in myotonic dystrophies : a model of premature aging. **7,** 1–16 (2015).

2. Meola, G. & Cardani, R. Myotonic dystrophies: An update on clinical aspects, genetic, pathology, and molecular pathomechanisms. *Biochim. Biophys. Acta - Mol. Basis Dis.* **1852,** 594–606 (2015).

3. Siciliano, G., Ml, M., Gennarelli, M., Angelini, C. & Rocchi, A. Epidemiology of myotonic dystrophy in Italy : re-apprisal after genetic diagnosis. 344–349 (2001).

4. Yotova, V. *et al.* Anatomy of a founder effect : myotonic dystrophy in Northeastern Quebec. 177–187 (2005). doi:10.1007/s00439-005-1298-8

5. Thornton, C. A. Myotonic Dystrophy. *Neurol. Clin.* **32,** 705–719 (2014).

6. Udd, B. *et al.* 140th ENMC International Workshop: Myotonic Dystrophy DM2/PROMM and other myotonic dystrophies with guidelines on management. *Neuromuscul. Disord.* **16,** 403–413 (2006).

7. Turner, C. & Hilton-Jones, D. Myotonic dystrophy: diagnosis, management and new therapies. *Curr. Opin. Neurol.* **27,** 599–606 (2014).

8. IDMC. New nomenclature and DNA testing guidelines for myotonic dystrophy type 1 (DM1)-The international consortium meeting-. **1,** 1218–1221 (2000).

9. Harper, P. S. Congenital myotonic dystrophy in Britain. (1975).

10. Liquori, C. L. *et al.* Myotonic Dystrophy Type 2 Caused by a CCTG Expansion in Intron 1 of ZNF9. **293,** 0–4 (2001).

11. Meola, G. Clinical aspects, molecular pathomechanisms and management of myotonic dystrophies. *Acta Myol.* **32,** 154–65 (2013).

12. Schneider, C. *et al.* Proximal myotonic myopathy. (2000).

13. Temmerman, N. De *et al.* Intergenerational Instability of the Expanded CTG Repeat in the DMPK Gene : Studies in Human Gametes and Preimplantation Embryos. **1995,** 325–329 (2004).

14. Smeets, M., Loots, W., Anten, H. B. M., Mirandolle, J. F. & Geraedts, P. M. Paternal transmission of congenital myotonic dystrophy. 930–933 (1997).

15. Die, C. E. M. De *et al.* Influence of Sex of the Transmitting Parent as Well of Parental Allele Size on the CTG Expansion in Myotonic Dystrophy (DM) as. 1016–1023 (1993).

16. Day, J. W. *et al.* Myotonic dystrophy type 2 Molecular , diagnostic and clinical spectrum. (2003).

17. Flachenecker, P. *et al.* Assessment of cardiovascular autonomic function in myotonic dystrophy type 2 (DM2 / PROMM). **13,** 289–293 (2003).

18. Gadalla, S. M. *et al.* Quantifying Cancer Absolute Risk and Cancer Mortality in the Presence of Competing Events after a Myotonic Dystrophy Diagnosis. **8,** 1–7 (2013).

19. Win, A. K., Perattur, P. G., Pulido, J. S., Pulido, C. M. & Lindor, N. M. Increased Cancer Risks in Myotonic Dystrophy. *JMCP* **87,** 130–135 (2012).

20. Fernández-Torrón, R., Mikel García-Puga, J.-I. E., Miren Maneiro, Ana-María Cobo, Juan-José Poza, J.-B. E. & Miren Zulaica, Irune Ruiz, Loreto Martorell, David Otaegui, Ander Matheu, A. L. de M. Cancer risk in DM1 is sex-related and linked to miRNA-200/141 downregulation. *Neurology* **87,** 1250–1257 (2016).

21. Heatwole, C. R. . M. J. M. B. M. R. T. I. Laboratory Abnormalities in Ambulatory Patients With Myotonic Dystrophy Type 1. **63,** 1149–1153 (2006).

22. Pan, H. *et al.* Increased (CTG / CAG) n lengths in myotonic dystrophy type 1 and Machado – Joseph disease genes in idiopathic azoospermia patients. **17,** 1578–1583 (2002).

23. Verpoest, W. *et al.* The reproductive outcome of female patients with myotonic dystrophy type 1 (DM1) undergoing PGD is not affected by the size of the expanded CTG repeat tract. **1,** 327–333 (2010).

24. Srebnik, N., Margalioth, E. J., Rabinowitz, R. & Varshaver, I. Ovarian reserve and PGD treatment outcome in women with myotonic dystrophy. *Reprod. Biomed. Online* **29,** 94–101 (2014).

25. Osborne, R. J. & Thornton, C. A. RNA-dominant diseases. **15,** 162–169 (2006).

26. Klein, a F., Gasnier, E. & Furling, D. Gain of RNA function in pathological cases: Focus on

myotonic dystrophy. *Biochimie* **93,** 2006–12 (2011).

27. Day, J. W. & Ranum, L. P. W. RNA pathogenesis of the myotonic dystrophies. *Neuromuscul. Disord.* **15,** 5–16 (2005).

28. Pascual, M., Vicente, M., Monferrer, L. & Artero, R. The Muscleblind family of proteins: An emerging class of regulators of developmentally programmed alternative splicing. *Differentiation* **74,** 65–80 (2006).

29. Davis BM, McCurrach ME, Taneja KL, Singer RH, Housman, D. Expansion of a CUG trinucleotide repeat in the 3 □ untranslated region of myotonic dystrophy protein kinase transcripts results. *Proc. Natl. Acad. Sci.* **94,** 7388–7393 (1997).

30. Taneja KL, McCurrach M, Schalling M, Housman D, S. R. Foci of Trinucleotide Repeat Transcripts in Nuclei of Myotonic Dystrophy Cells and Tissues. **128,** 995–1002 (1995).

31. Harmon, E. B. *et al.* Myotonic dystrophy protein kinase is critical for nuclear envelope integrity. *J. Biol. Chem.* **286,** 40296–40306 (2011).

32. Harmon, E. B., Harmon, M. L., Larsen, T. D., Paulson, A. F. & Perryman, M. B. Myotonic dystrophy protein kinase is expressed in embryonic myocytes and is required for myotube formation. *Dev. Dyn.* **237,** 2353–2366 (2008).

33. Murányi, A. *et al.* Myotonic dystrophy protein kinase phosphorylates the myosin phosphatase targeting subunit and inhibits myosin phosphatase activity. *FEBS Lett.* **493,** 80–84 (2001).

34. Margarit E, Armas P, García Siburu N, C. N. CNBP modulates the transcription of Wnt signaling pathway components. *Biochim. Biophys. Acta* **1839,** 1151–1160 (2014).

35. Rudnicki M.A., W. B. O. Wnt signaling in bone and muscle. *Bone* **80,** 60–66 (2015).

36. Jansen G., Groenen P., Bächner D., Jap P.H.K, Coerwinkel M., Oerlemans F., van den Broek W., Gohlsch B., Pette D., Plomp J.J., Molenaar P.C., Nederhoff M.G.J., van Echteld C.J.A., Dekker M., Berns A., Hameister H., W. B. Abnormal myotonic dystrophy protein kinase levels produce only mild myopathy in mice. *Nat. Genet.* **13,** 316–324 (1996).

37. Reddy S., Smith D.B.J., Rich M.M., Leferovich J.M., Reilly P., Davis B.M., Tran K., Rayburn H., Bronson R., Cros D., Balice-Gordon R.J., H. D. Mice lacking the myotonic dystrophy protein kinase develop a late onset progressive myopathy. *Nat. Genet.* **13,** 325–

335 (1996).

38. Chen W., Wang Y., Abe Y., Cheney L., Udd B., Li, Y. P. Haploinsuffciency for Znf9 in Znf9+/− Mice Is Associated with Multiorgan Abnormalities Resembling Myotonic Dystrophy. *J. Mol. Biol.* **368,** 8–17 (2007).

39. Margolis J.M.Schoser B.G., Moseley M.L., Day J., R. L. P. DM2 intronic expansions: evidence for CCUG accumulation without flanking sequence or effects on ZNF9 mRNA processing or protein expression. *Hum. Mol. Genet.* **15,** 1808–1815 (2006).

40. Ho, T. H. *et al.* Muscleblind proteins regulate alternative splicing. *EMBO J.* **23,** 3103–12 (2004).

41. Wang, E. T. *et al.* Transcriptome-wide Regulation of Pre-mRNA Splicing and mRNA Localization by Muscleblind Proteins. **150,** 710–724 (2013).

42. Kalsotra, A. *et al.* A postnatal switch of CELF and MBNL proteins reprograms alternative splicing in the developing heart BIOLOGY. **41,** 1–6 (2008).

43. Lin, X. *et al.* Failure of MBNL1-dependent post-natal splicing transitions in myotonic dystrophy. *Hum. Mol. Genet.* **15,** 2087–97 (2006).

44. Mankodi, A. *et al.* Expanded CUG Repeats Trigger Aberrant Splicing of ClC-1 Chloride Channel Pre-mRNA and Hyperexcitability of Skeletal Muscle in Myotonic Dystrophy. **10,** 35–44 (2002).

45. Savkur, R. S., Philips, a V & Cooper, T. a. Aberrant regulation of insulin receptor alternative splicing is associated with insulin resistance in myotonic dystrophy. *Nat. Genet.* **29,** 40–7 (2001).

46. Philips, A.V., Timchenko L.T., C. T. A. Disruption of Splicing Regulated by a CUG-Binding Protein in Myotonic Dystrophy. *Science (80-.).* **280,** 737–741 (1998).

47. Nakamori, M. *et al.* Splicing biomarkers of disease severity in myotonic dystrophy. *Ann. Neurol.* **74,** 862–72 (2013).

48. Perfetti, A. *et al.* Genome Wide Identification of Aberrant Alternative Splicing Events in Myotonic Dystrophy Type 2. **9,** (2014).

49. Zu, T. *et al.* Non-ATG – initiated translation directed by microsatellite expansions. 1–6

(2010). doi:10.1073/pnas.1013343108/-/DCSupplemental.www.pnas.org/cgi/doi/10.1073/pnas.1013343108

50. Udd, B. & Krahe, R. The myotonic dystrophies: molecular, clinical, and therapeutic challenges. *Lancet Neurol.* **11,** 891–905 (2012).

51. Tian, B. *et al.* Expanded CUG repeat RNAs form hairpins that activate the double-stranded RNA-dependent protein kinase PKR. *RNA* **6,** 79–87 (2000).

52. Halliday D, Ford GC, Edwards RH, Rennie MJ, G. R. In vivo estimation of muscle protein synthesis in myotonic dystrophy. *Ann. Neurol.* **17,** 65–69 (1985).

53. Huichalaf, C. *et al.* Reduction of the rate of protein translation in patients with myotonic dystrophy 2. *J Neurosci* **29,** 9042–9049 (2009).

54. Warner, J. P. *et al.* A general method for the detection of large CAG. 1022–1026 (1996).

55. Kakourou, G. *et al.* Modification of the triplet repeat primed polymerase chain reaction method for detection of the CTG repeat expansion in myotonic dystrophy type 1 : application in preimplantation genetic diagnosis. *Fertil. Steril.* **94,** 1674–1679 (2010).

56. Catalli, C., Morgante, A., Iraci, R., Rinaldi, F. & Botta, A. Validation of Sensitivity and Specificity of Tetraplet-Primed PCR (TP-PCR) in the Molecular Diagnosis of Myotonic Dystrophy Type 2 (DM2). *J. Mol. Diagnostics* **12,** 601–606 (2010).

57. Bachinski, L. L. *et al.* Confirmation of the Type 2 Myotonic Dystrophy (CCTG) n Expansion Mutation in Patients with Proximal Myotonic Myopathy / Proximal Myotonic Dystrophy of Different European Origins : A Single Shared Haplotype Indicates an Ancestral Founder Effect. **1,** 835–848 (2003).

58. Cardani, R., Mancinelli, E., Sansone, V., Rotondo, G. & Meola, G. Biomolecular identification of (CCTG)n mutation in myotonic dystrophy type 2 (DM2) by FISH on muscle biopsy. *Eur. J. Histochem.* **48,** 437–442 (2004).

59. Sallinen, R. *et al.* New methods for molecular diagnosis and demonstration of the (CCTG)n mutation in myotonic dystrophy type 2 (DM2). *Neuromuscul. Disord.* **14,** 274–283 (2004).

60. Pasquinelli, A. A. MicroRNAs and their targets: recognition, regulation and an emerging reciprocal relationship. *Nat. Rev. Genet.* **13,** 271–282 (2012).

61. Friedman, R. C., Farh, K. K. H., Burge, C. B. & Bartel, D. P. Most mammalian mRNAs are conserved targets of microRNAs. *Genome Res.* **19,** 92–105 (2009).

62. Finnegan, E. F. & Pasquinelli, A. E. MicroRNA biogenesis: regulating the regulators. *Crit. Rev. Biochem. Mol. Biol.* **48,** 51–68 (2013).

63. Lee, Y. *et al.* MicroRNA genes are transcribed by RNA polymerase II. *Embo J* **23,** 4051–4060 (2004).

64. Winter J., Jung S., Keller S., Gregory R.I., D. S. Many roads to maturity: microRNA biogenesis pathways and their regulation. *Nat. Cell Biol.* **11,** 228–234 (2009).

65. Lee Y., Ahn C., Han J., Choi H., Kim J., Yim J., Lee J., Provost P., Radmark O., Kim S., K. N. The nuclear RNase III Drosha initiates microRNA processing. *Nature* **425,** 415–419 (2003).

66. Yi, R., Qin, Y., Macara, I. G. & Cullen, B. R. Exportin-5 mediates the nuclear export of pre-microRNAs and short hairpin RNAs. *Genes Dev.* **17,** 3011–3016 (2003).

67. Jinek M., D. J. A. A three-dimensional view of the molecular machinery of RNA interference. *Nature* **457,** 405–412 (2009).

68. Lewis, B. P., Shih, I., Jones-Rhoades, M. W., Bartel, D. P. & Burge, C. B. Prediction of Mammalian MicroRNA Targets. *Cell* **115,** 787–798 (2003).

69. Thomson, D. W., Bracken, C. P. & Goodall, G. J. Experimental strategies for microRNA target identification. *Nucleic Acids Res.* **39,** 6845–6853 (2011).

70. Fasanaro, P. *et al.* An integrated approach for experimental target identification of hypoxia-induced miR-210. *J. Biol. Chem.* **284,** 35134–35143 (2009).

71. Tay Yvonne, Zhang Jinqiu, Thomson Andrew M., Lim Bing, R. I. MicroRNAs to Nanog, Oct4 and Sox2 coding regions modulate embryonic stem cell differentiation. *Nature* **455,** 1124–1128 (2008).

72. Huntzinger E., I. E. Gene silencing by microRNAs: contributions of translational repression and mRNA decay. *Nat. Rev. Genet.* **12,** 99–110 (2011).

73. Gebauer F., H. M. W. Molecular mechanisms of translational control. *Nat. Rev. Mol. Cell Biol.* **5,** 827–835 (2004).

74. Humphreys, D. T., Westman, B. J., Martin, D. I. K. & Preiss, T. MicroRNAs control translation initiation by inhibiting eukaryotic initiation factor 4E/cap and poly(A) tail function. *Proc. Natl. Acad. Sci. U. S. A.* **102,** 16961–6 (2005).

75. Pillai, R. S. Inhibition of Translational Initiation by Let-7 MicroRNA in Human Cells. *Science (80-.).* **309,** 1573–1576 (2005).

76. Filipowicz W., Bhattacharyya S.N., S. N. Mechanisms of post-transcriptional regulation by microRNAs: are the answers in sight? *Nat. Rev. Genet.* **9,** 102–114 (2008).

77. Mathonnet, G. *et al.* MicroRNA Inhibition of Translation. *Science (80-.).* **317,** 1764–1767 (2007).

78. Nottrott S., Simard M.J., R. J. D. Human let-7a miRNA blocks protein production on actively translating polyribosomes. *Nat. Struct. Mol. Biol.* **13,** 1108–1114 (2006).

79. Petersen, C. P., Bordeleau, M. E., Pelletier, J. & Sharp, P. A. Short RNAs repress translation after initiation in mammalian cells. *Mol. Cell* **21,** 533–542 (2006).

80. Chekulaeva, M. *et al.* miRNA repression involves GW182-mediated recruitment of CCR4–NOT through conserved W-containing motifs. *Nat. Struct. Mol. Biol.* **18,** 1218–1226 (2011).

81. Braun, J. E., Huntzinger, E., Fauser, M. & Izaurralde, E. GW182 proteins directly recruit cytoplasmic deadenylase complexes to miRNA targets. *Mol. Cell* **44,** 120–133 (2011).

82. Fabian MR, Svitkin YV, S. N. An efficient system for let-7 microRNA and GW182 protein-mediated deadenylation in vitro. *Methods Mol. Biol.* **725,** 207–217 (2011).

83. Fabian Marc R., S. N. The mechanics of miRNA-mediated gene silencing: a look under the hood of miRISC. *Nat. Struct. Mol. Biol.* **19,** 586–593 (2012).

84. Vasuvedan S., Tong Y., S. J. A. Switching from Repression to Activation: MicroRNAs Can Up-Regulate Translation. *Science* 1931–1934 (2007).

85. Kim, D. H., Saetrom, P., Snøve, O. & Rossi, J. J. MicroRNA-directed transcriptional gene silencing in mammalian cells. *Proc. Natl. Acad. Sci. U. S. A.* **105,** 16230–5 (2008).

86. Bartel, D. P. MicroRNAs: target recognition and regulatory functions. *Cell* **136,** 215–33 (2009).

87. Makarova J.A., Shkurinov M.U., Turchinovich A.A., Tonevitsky A.G., G. A. I. Circulating

microRNAs. *Biochemistry* **80,** 11171126 (2015).

88. Landgraf, P. *et al.* A Mammalian microRNA Expression Atlas Based on Small RNA Library Sequencing. *Cell* **129,** 1401–1414 (2007).

89. Lagos-Quintana, M. *et al.* Identification of tissue-specific MicroRNAs from mouse. *Curr. Biol.* **12,** 735–739 (2002).

90. Guo, Z. *et al.* Genome-wide survey of tissue-specific microRNA and transcription factor regulatory networks in 12 tissues. *Sci. Rep.* **4,** 5150 (2014).

91. Falcone, G., Perfetti, A., Cardinali, B. & Martelli, F. Noncoding RNAs: Emerging players in muscular dystrophies. *Biomed Res. Int.* **2014,** 503634 (2014).

92. Horak, M., Novak, J. & Bienertova-Vasku, J. Muscle-specific microRNAs in skeletal muscle development. *Dev. Biol.* **410,** 1–13 (2016).

93. Eisenberg, I. *et al.* Distinctive patterns of microRNA expression in primary muscular disorders. *Proc. Natl. Acad. Sci. U. S. A.* **104,** 17016–17021 (2007).

94. Fernandez-Costa, J. M. *et al.* Expanded CTG repeats trigger miRNA alterations in Drosophila that are conserved in myotonic dystrophy type 1 patients. *Hum. Mol. Genet.* **22,** 704–716 (2013).

95. Gambardella, S. *et al.* Overexpression of microRNA-206 in the skeletal muscle from myotonic dystrophy type 1 patients. *J. Transl. Med.* **8,** 48 (2010).

96. Perbellini, R. *et al.* Dysregulation and cellular mislocalization of specific miRNAs in myotonic dystrophy type 1. *Neuromuscul. Disord.* **21,** 81–88 (2011).

97. Cardinali, B. *et al.* MicroRNA-222 regulates muscle alternative splicing through Rbm24 during differentiation of skeletal muscle cells. *Cell Death Dis.* **7,** e2086 (2016).

98. Weickmann, J. L. & Glitz, D. G. Human ribonucleases. Quantitation of pancreatic-like enzymes in serum, urine, and organ preparations. *J. Biol. Chem.* **257,** 8705–8710 (1982).

99. Etheridge, A., Lee, I., Hood, L., Galas, D. & Wang, K. Extracellular microRNA: A new source of biomarkers. *Mutat. Res. - Fundam. Mol. Mech. Mutagen.* **717,** 85–90 (2011).

100. Vickers, K. C., Palmisano, B. T., Shoucri, B. M., Shamburek, R. D. & Remaley, A. T. MicroRNAs are transported in plasma and delivered to recipient cells by high-density

lipoproteins. **13,** 423–433 (2011).

101. Boon, R. A. & Vickers, K. C. Intercellular transport of MicroRNAs. *Arterioscler. Thromb. Vasc. Biol.* **33,** 186–192 (2013).

102. Mitchell, P. S. *et al.* Circulating microRNAs as stable blood-based markers for cancer detection. *Proc. Natl. Acad. Sci. U.S.A.* **105,** 10513–10518 (2008).

103. Corsten, M. F. *et al.* Circulating MicroRNA-208b and MicroRNA-499 reflect myocardial damage in cardiovascular disease. *Circ. Cardiovasc. Genet.* **3,** 499–506 (2010).

104. D'Alessandra, Y. *et al.* Circulating microRNAs are new and sensitive biomarkers of myocardial infarction. *Eur. Heart J.* **31,** 2765–2773 (2010).

105. Mizuno, H. *et al.* Identification of Muscle-Specific MicroRNAs in Serum of Muscular Dystrophy Animal Models: Promising Novel Blood-Based Markers for Muscular Dystrophy. *PLoS One* **6,** e18388 (2011).

106. Zaharieva, I. T. *et al.* Dystromirs as serum biomarkers for monitoring the disease severity in Duchenne muscular Dystrophy. *PLoS One* **8,** e80263 (2013).

107. Koutsoulidou, A. *et al.* Elevated Muscle-Specific miRNAs in Serum of Myotonic Dystrophy Patients Relate to Muscle Disease Progress. *PLoS One* **10,** e0125341 (2015).

108. Perfetti, A. *et al.* Plasma microRNAs as biomarkers for myotonic dystrophy type 1. *Neuromuscul. Disord.* **24,** 509–15 (2014).

109. Creemers, E. E., Tijsen, A. J. & Pinto, Y. M. Circulating MicroRNAs. *Circ. Res.* **110,** 483–495 (2012).

110. Vester, B. & Wengel, J. Current Topics LNA (Locked Nucleic Acid): High-Affinity Targeting of Complementary. *October* **43,** 13233–41 (2004).

111. Jopling, C. L., Yi, M., Lancaster, A. M., Lemon, S. M. & Sarnow, P. Modulation of hepatitis C virus RNA abundance by a liver-specific MicroRNA. *Science* **309,** 1577–81 (2005).

112. Haussecker, D. & Kay, M. a. miR-122 continues to blaze the trail for microRNA therapeutics. *Mol. Ther.* **18,** 240–242 (2010).

113. Valaperta, R. *et al.* Identification and characterization of DM1 patients by a new diagnostic certified assay: Neuromuscular and cardiac assessments. *Biomed Res. Int.* **2013,** 1–6 (2013).

114. Mathieu, J., Boivin, H., Meunier, D., Gaudreault, M. & Bégin, P. Assessment of a disease-specific muscular impairment rating scale in myotonic dystrophy. *Neurology* **56,** 336–40 (2001).

115. Compston, A. Aids to the investigation of peripheral nerve injuries. Medical Research Council: Nerve Injuries Research Committee. His Majesty's Stationery Office: 1942; pp. 48 (iii) and 74 figures and 7 diagrams. *Brain* **133,** 2838–2844 (2010).

116. Kroll M.H., M. R. *Endogenous Interferences in Clinical Laboratory Tests*. *Eds de Gruyter, Ch.3* (Walter de Gruyter, 2013).

117. Livak, K. J. & Schmittgen, T. D. Analysis of relative gene expression data using real-time quantitative PCR and the 2-ΔΔCT method. *Methods* **25,** 402–408 (2001).

118. Li, H. & Durbin, R. Fast and accurate short read alignment with Burrows-Wheeler transform. *Bioinformatics* **25,** 1754–1760 (2009).

119. Law, C. W., Chen, Y., Shi, W. & Smyth, G. K. voom: precision weights unlock linear model analysis tools for RNA-seq read counts. *Genome Biol.* **15,** R29 (2014).

120. Robinson J.T, Thorvaldsdóttir H., Winckler W., Guttman M., Lander E.S., Getz G., M. J. P. Integrative Genomics Viewer. *Nat. Biotechnol.* **29,** 24–26 (2011).

121. Henderson, A. Assessing test accuracy and its clinical consequences: a primer for receiver operating characteristic curve analysis. *Annu. Clin. Biochem.* **30,** 521–539 (1993).

122. Hanley, a, Mcneil, J. & Ph, D. under a Receiver Characteristic. *Radiology* **143,** 29–36 (1982).

123. Greiner, M., Pfeiffer, D. & Smith, R. . Principles and practical application of the receiver-operating characteristic analysis for diagnostic tests. *Prev. Vet. Med.* **45,** 23–41 (2000).

124. R Core Team (2013). R: a language and environment for statistical computing. R foundation for statistical computing, Vienna, Austria. URL https://www.r-project.org/.

125. Marabita, F. *et al.* Normalization of circulating microRNA expression data obtained by quantitative real-time RT-PCR. **17,** 204–212 (2016).

126. Backes, C., Keller, A., Kuentzer, J., Kneissl, B., Comtesse, N., Elnakady, Y.A., Müller, R., Meese, E., and Lenhof, H. P. GeneTrail - advanced gene set enrichment analysis. *Nucleic*

Acid Res. (2007). doi:10.1093/nar/gkm323

127. Figeac, N., Serralbo, O., Marcelle, C. & Zammit, P. S. ErbB3 binding protein-1 (Ebp1) controls proliferation and myogenic differentiation of muscle stem cells. *Dev. Biol.* **386,** 135–151 (2014).

128. Sepulveda, P. V *et al.* Evaluation of follistatin as a therapeutic in models of skeletal muscle atrophy associated with denervation and tenotomy. *Sci. Rep.* **5,** 17535 (2015).

129. Moll, R. *et al.* The cardiac isoform of ??-actin in regenerating and atrophic skeletal muscle, myopathies and rhabdomyomatous tumors: An immunohistochemical study using monoclonal antibodies. *Virchows Arch.* **449,** 175–191 (2006).

130. Gao, Z. & Cooper, T. A. Reexpression of pyruvate kinase M2 in type 1 myofibers correlates with altered glucose metabolism in myotonic dystrophy. *Proc. Natl. Acad. Sci. U. S. A.* **110,** 13570–5 (2013).

131. Alvim, R. O., Cheuhen, M. R., Machado, S. R., Sousa, A. G. P. & Santos, P. C. J. L. General aspects of muscle glucose uptake. *An. Acad. Bras. Cienc.* **87,** 351–368 (2015).

132. Rau, F. *et al.* Misregulation of miR-1 processing is associated with heart defects in myotonic dystrophy. *Nat. Struct. Mol. Biol.* **18,** 840–845 (2011).

133. Stadler, P. F. *et al.* Evolution of Vault RNAs. *Mol. Biol. Evol.* **26,** 1975–1991 (2009).

134. Dogan, C. *et al.* Gender as a Modifying Factor Influencing Myotonic Dystrophy Type 1 Phenotype Severity and Mortality: A Nationwide Multiple Databases Cross-Sectional Observational Study. *PLoS One* **11,** e0148264 (2016).

135. Dai, A. *et al.* MicroRNA-133b stimulates ovarian estradiol synthesis by targeting. *FEBS Lett.* **587,** 2474–2482 (2013).

136. Harafuji, N., Schneiderat, P., Walter, M. C. & Chen, Y. miR-411 is up-regulated in FSHD myoblasts and suppresses myogenic factors. **4,** 12–16 (2013).

137. Kota, J. *et al.* Follistatin Gene Delivery Enhances Muscle Growth and Strength in Nonhuman Primates. **1,** 1–17 (2010).

138. Nakatani, M. *et al.* Transgenic expression of a myostatin inhibitor derived from follistatin increases skeletal muscle mass and ameliorates dystrophic pathology in mdx mice. *FASEB J.*

22, 477–487 (2008).

139. Davey, J. R. *et al.* Integrated expression analysis of muscle hypertrophy identifies Asb2 as a negative regulator of muscle mass. *JCI insight* **1,** 1–15 (2016).

140. Cardinali, B. *et al.* Microrna-221 and microrna-222 modulate differentiation and maturation of skeletal muscle cells. *PLoS One* **4,** (2009).

141. Ford B.D., Han B., F. G. D. Differentiation-dependent regulation of skeletal myogenesis by neuregulin-1. *Biochem. Biophys. Res. Commun.* **306,** 276–281 (2003).

142. Hellyer, N., Mantilla, C., Park, E., Zhan, W. & Sieck, G. Neuregulin-dependent protein synthesis in C2C12 myotubes and rat diaphragm muscle. *Am. Hournal Physiol. Cell Physiol.* **291,** C1056–C1061 (2006).

143. Kim, D. *et al.* Neuregulin stimulates myogenic differentiation in an autocrine manner. *J. Biol. Chem.* **274,** 15395–15400 (1999).

144. Beermann, J. *et al.* Non-coding RNAs in Development and Disease: Background, Mechanisms, and Therapeutic Approaches. *Physiol. Rev.* **96,** 1297–325 (2016).

145. Kang, Y. *et al.* Combinations of kinase inhibitors protecting myoblasts against hypoxia. *PLoS One* **10,** 1–16 (2015).

146. Chaillou, T. & Lanner, J. T. Regulation of myogenesis and skeletal muscle regeneration: effects of oxygen levels on satellite cell activity. *FASEB J.* **30,** 1–14 (2016).

147. Di Carlo, A. *et al.* Hypoxia Inhibits Myogenic Differentiation through Accelerated MyoD Degradation. *J. Biol. Chem.* **279,** 16332–16338 (2004).

148. Buckingham M, Alonso S, Barton P, Cohen A, Daubas P, Garner I, Robert B, W. A. Actin and myosin multigene families: their expression during the formation and maturation of striated muscle. *Am J Med Genet.* **25,** 623–634 (1986).

149. Thornell, L.-E. *et al.* Satellite cell dysfunction contributes to the progressive muscle atrophy in myotonic dystrophy type 1. *Neuropathol. Appl. Neurobiol.* **35,** 603–613 (2009).

150. Nascimento, E. B., Osler, M. E. & Zierath, J. R. Sestrin 3 regulation in type 2 diabetic patients and its influence on metabolism and differentiation in skeletal muscle. *Am. J. Physiol. Endocrinol. Metab.* **305,** E1408-14 (2013).

151. Timchenko, L. Molecular mechanisms of muscle atrophy in myotonic dystrophies. *Int. J. Biochem. Cell Biol.* (2013). doi:10.1016/j.biocel.2013.06.010

152. Kumarswamy, R. & Thum, T. Non-coding RNAs in cardiac remodeling and heart failure. *Circ. Res.* **113,** 676–689 (2013).